ABSTRACT

BOWKER, COLLEEN KATHERINE. Assessment of Microbial UV Fluence-Response using a Novel UV-LED Collimated Beam Apparatus. (Under the direction of Joel J. Ducoste).

The use of ultraviolet (UV) light for disinfection applications has become increasingly popular due to the ability of UV to inactivate chlorine resistant microorganisms and disinfect without the production of known disinfection by-products. The most widely used UV light sources are low- and medium-pressure mercury lamps. Technology that has recently become available is UV light emitting diodes (UV-LEDs) with emission wavelengths in the germicidal range. UV-LEDs do not contain toxic mercury, offer design flexibility due to their small size, and have a longer operational life than mercury lamps. This research sought to determine the UV fluence-response of several target non-pathogenic microorganisms to UV-LEDs by performing collimated beam tests. Comsol Multiphysics was utilized to create an optimal UV-LED collimated beam design based on number and spacing of UV-LEDs and distance of the sample from the light source while minimizing the overall cost. The optimized UV-LED collimated beam apparatus and a low-pressure mercury lamp collimated beam apparatus were used to determine the UV fluence-response of three surrogate microorganisms (*E. coli*, MS-2, *T7*) to 255 nm UV-LEDs, 275 nm UV-LEDs, and 254 nm low-pressure mercury lamps. Irradiation by low-pressure mercury lamps produced greater *E. coli* and MS-2 inactivation than 255 nm and 275 nm UV-LEDs and similar T7 inactivation to irradiation by 275 nm UV-LEDs. The 275 nm UV-LEDs produced more efficient T7 and *E. coli* inactivation than 255 nm UV-LEDs while both 255 nm and 275 nm UV-LEDs produced comparable microbial inactivation for MS-2.

Assessment of Microbial UV Fluence-Response using a Novel UV-LED Collimated Beam Apparatus

by
Colleen Bowker

A thesis submitted to the Graduate Faculty of
North Carolina State University
in partial fulfillment of the
requirements for the degree of
Master of Science

Civil Engineering

Raleigh, North Carolina

2010

APPROVED BY:

_____	_____
Joel J. Ducoste, PhD Committee Chair	Francis de los Reyes, PhD

_____

Detlef R. U. Knappe, PhD

DEDICATION

To Corey.

Thank you for always making me smile.

BIOGRAPHY

Colleen was born and raised in Charlotte, NC. She completed her undergraduate degree in Environmental Engineering at North Carolina State University and pursued a Master of Science in Civil Engineering at North Carolina State University under advisor Dr. Joel Ducoste.

ACKNOWLEDGMENTS

I would like to thank the following people that have helped and supported me during the completion of this degree:

My fellow Dungeon Dwellers: Erin Gallimore, Tarek Aziz, Tony Sobremisana, Scott Alpert, and Rupa Iasmin. Thank you for your support and excellent listening skills.

The students who helped with the research: Amanda Sain, Susan Dunn, Karthik Sundaramoorthy, and Rony Sarafin.

My committee: Dr. Ducoste, Dr. de los Reyes, and Dr. Knappe. It was a privilege to have learned from all of you.

Zuzana Bohrerova and Mark Jason So for guiding me through the microbiological techniques.

Sensor Electronic Technology, Inc. for providing the UV-LEDs and Clancy Environmental Consultants for providing the T7 bacteriophage.

The National Science Foundation for funding the research and me!

My family: Mom, Dad, Megan, Corey, and Picasso. I love you.

TABLE OF CONTENTS

LIST OF TABLES

LIST OF FIGURES

1. INTRODUCTION

The use of ultraviolet (UV) light in drinking water disinfection applications has become a growing alternative to chemical disinfectants since its determination as an effective method for inactivating chlorine resistant pathogenic organisms without the production of any known disinfection by-products (Bohrerova et al., 2006). The majority of UV disinfection systems currently use low- or medium-pressure mercury lamps, which are toxic (contain mercury), require significant amounts of energy, and have a short lifetime. Other alternative UV light emission sources have been developed (Wang et al., 2005; Bohrerova et al., 2008). A possible alternative to UV mercury lamps or alternative UV emission sources is the use of UV light emitting diodes (UV-LEDs), which contain no known toxic elements that can be released upon breakage, have a much longer lifetime, and provide design flexibility due to their small size (Shur and Gaska, 2008). Recent advances in technology have allowed the production of UV-LEDs with emission wavelengths in the germicidal range, with the shortest wavelength at 237 nm (Shur and Gaska, 2008). However, little research has been completed that assesses the disinfection efficiency of UV-LEDs.

The purpose of this study was to determine the response of target non-pathogenic microorganisms to UV-LEDs by performing detailed collimated beam tests. This research will be an important component in studies that seek to design an optimal UV-

LED reactor through validation by biodosimetry experiments.

2. BACKGROUND

2.1 UV DISINFECTION

UV disinfection involves the delivery of UV light with germicidal properties to pathogens. The UV spectrum spans wavelengths from 100 to 400 nm. However, UV disinfection usually occurs in the UVC (200 to 280 nm) and UVB (280 to 315 nm) regions due to their germicidal efficiency (USEPA, 2006). The mechanism of UV disinfection is to prevent microorganisms from replicating by damaging their nucleic acid. During this process, pyrimidine bases in DNA or RNA absorb UV light, which produces a photochemical reaction. One result of this reaction can be a chemical dimer that bonds two pyrimidine bases, preventing the formation of new nucleic acid chains (Bolton and Linden, 2003). Other less common forms of damage are pyrimidine (6-4) pyrimidone photoproducts and protein-DNA cross-links (USEPA, 2006).

2.2 UV LIGHT EMISSION TECHNOLOGIES

Several alternative UV light emitting technologies have been developed for disinfection processes. These include low-pressure, low-pressure high-output, medium pressure, pulsed UV, and UV-LEDs. Other technologies may exist as research in this area is ongoing. In low-pressure (LP-UV) lamps, UV light is emitted from the electrical current flow through the mercury vapor between the lamp electrodes. Low-pressure

mercury vapor lamps produce the majority of their UV output at 254 nm, which is close to the wavelengths most effective in the inactivation of microorganisms (i.e., 260 – 265 nm). LPHO-UV lamps emit monochromatic radiation also at 254 nm with a slightly higher intensity (USEPA, 2006).

Medium pressure (MP-UV) lamps are mercury-arc lamps that operate at much higher pressures (i.e., a million times the pressure) and higher temperatures than LP-UV lamps. The increased pressure causes emission of significantly higher intensity radiation and broader emission lines. The emission from a MP lamp is polychromatic over a broad range of wavelengths (i.e., 185 nm to 1,000 nm). Unfortunately, only approximately 15 to 20 percent of the polychromatic radiation is emitted in the germicidal range (200-300 nm). Although MP-UV lamps have a lower germicidal efficiency per unit of power input than LP-UV lamps, MP-UV lamps can emit hundreds of times the germicidal irradiance of LP-UV lamps. This higher emittance means that a relatively smaller footprint can be used for MP-UV disinfection system (USEPA, 2006)

Pulsed UV (PUV) sources, a relatively new technology, emit intense flashes of white light with wavelengths from 200 nm to 1000 nm. Each pulse may produce a UV intensity much larger than the intensity produced by the sun at sea level and may only last a fraction of a second (Chung et al., 2008). PUV lamps do not contain mercury, turn on instantly, and discharge a non-toxic rare gas, such as xenon or krypton. Pulsed lamps can exist as either flash-lamp type, employing constrained discharges within a small tube or

surface discharge (SD) type, using a plasma discharge external to a dielectric material enclosed within a large diameter tube (Bohrerova et al., 2008). An ongoing debate has occurred over the comparative inactivation efficiency of continuous and PUV sources. While some studies have reported more effective inactivation using PUV sources, others have reported no difference between the two (Wang et al., 2005).

Light-emitting diodes (LEDs) are created by connecting two semiconductors known as p-type and n-type that move electrons into positively charged holes between these two materials. Light is generated when the electrons and holes collide at a junction. The wavelength of light will depend on the type of material used for the two semiconductors (i.e., indium gallium nitride for light in the visible range and aluminium gallium nitride and aluminium nitride for ultraviolet light) (Dume, 2006). Recently, deep UV-LEDs with peak emission wavelength from 250 to 340 nm have been manufactured for many potential applications including microbial disinfection (Shur and Gaska, 2008). While mercury lamps only emit light at one wavelength (LP version) or multiple wavelengths simultaneously (MP version), UV-LEDs are capable of emitting light at different targeted wavelengths. Therefore, UV-LEDs are able to emit light at the exact peak of germicidal effectiveness for a particular organism (Shur and Gaska, 2008).

While other light sources may exist, UV-LEDs are potentially one of the best options for a UV disinfection light source because they do not contain toxic chemicals such as mercury and thus do not pose a potential disposal problem. Research is therefore needed to explore how a UV emission light source that is not limited to a cylindrical

geometry as with LP-, LPHO-, MP-, and PUV-lamps may improve the efficiency of UV-disinfection continuous-flow reactor designs.

2.3 BENCH SCALE COLLIMATED BEAM SYSTEMS

A bench scale collimated beam is commonly used to determine the UV fluence (or dose) response of a target microorganism (Bolton and Linden, 2003). A collimated beam apparatus consists of a UV light source that is directed onto a horizontal surface through a cylindrical tube or through consecutive apertures. The object to be irradiated is placed below the collimator on a horizontal platform that can be lowered or raised (Bolton and Linden, 2003). Other design characteristics include a shutter to control sample exposure times and a stir plate to ensure samples are evenly mixed during irradiation. Bolton and Linden introduced several correction factors that should be used when completing collimated beam experiments with a low-pressure UV lamp as the light source. These include the Petri factor, water factor, reflection factor, and divergence factor. The Petri factor is the ratio of the average irradiance for the entire area of the Petri dish to the irradiance at the middle of the dish. This factor allows for a more accurate reading of the average irradiance over the surface area of the sample. Bolton and Linden (2003) recommended a Petri factor equal to or greater than 0.9 for a well designed collimated beam apparatus. The water factor takes into account the decrease in light intensity caused by absorption in the water. The reflection factor accounts for refractive index changes when light passes through different media. The divergence

factor corrects for the divergence of the UV rays with increasing distance from the light source (Bolton and Linden, 2003). Like low-pressure mercury lamps, UV-LEDs emit mainly at one target wavelength. Therefore, these correction factors would also be applicable for UV-LED experiments. Other correction factors were also recommended for experiments using a medium pressure mercury lamp.

There are several challenges in designing a collimated beam apparatus based on a UV-LED light source. First, UV-LEDs are very small point sources, which make it difficult to create a uniform distribution of light across a sample surface. Second, as the UV-LED technology is still in the initial phase, the devices are very inefficient resulting in a low power output. Therefore, a number of UV-LEDs need to be used in a collimated beam apparatus in order to ensure a sufficient amount of light intensity is delivered to the sample. However, the UV-LEDs also need to be arranged in such a way to allow a uniform light distribution, which is characterized by the Petri factor. Finally, while utilizing a large number of UV-LEDs would be better to achieve a desired irradiance, each individual UV-LED is expensive. Therefore, there would be a need to optimally place the fewest number of UV-LEDs that would achieve a sufficient irradiance level at some distance within the collimated beam apparatus.

2.4 BIODOSIMETRY

The method presently used in UV reactor validation to determine the delivered UV fluence in a reactor is biodosimetry (USEPA, 2006). Biodosimetry involves spiking

a surrogate microorganism into the reactor influent flow and comparing the effluent microbial removal to a previously generated UV inactivation curve from bench-scale collimated beam tests. A single reduction equivalent dose (RED) can be generated to indicate one type of average UV dose in a reactor (USEPA, 2006).

2.5 PREVIOUS STUDIES WITH UV-LEDS

In one study, an attempt was made to develop a collimated beam apparatus that delivered uniform UV fluences from deep UV-LED arrays (Crawford et al., 2005). The final design included 2x2 element UV-LED arrays, with each element being 300 μm x 300 μm (Crawford et al., 2005). An intensity profile of the UV light emitted from the collimation tube showed an intensity variation of about 15 to 20% across the sample diameter and consequent failure of Bolton and Linden's (2003) recommendation for the Petri factor (Crawford et al, 2005). A high Petri factor is designed to minimize variation in incident irradiance over the sample surface area when computing the average irradiance.

In Crawford et al. (2005), the UV-LED collimated beam was used to conduct inactivation studies on *E. coli* strains ATCC 23229 and 15596 at 270 nm over a range of UV fluences. Due to low power output and absorption values, exposure times for the more resistant strain of *E. coli* ranged between 30 seconds and 10 minutes, with a maximum log kill of 1.89. The study resulted in much lower *E. coli* inactivation than

was expected and the need was expressed for further exposure studies. The low disinfection rates shown in this study were most likely due to low power outputs from the UV-LEDs. UV-LED power inefficiency was listed as a constraint for UV-LED applicability in Shur and Gaska (2008), but it was also mentioned that efficiency may soon be improved by an order of magnitude or more.

Another study that investigated using UV-LEDs for disinfection was Mori et al. (2007) in which *E. coli* DH5α was exposed to irradiation from a sterilization device that connected 8 UVA LEDs emitting a 365 nm wavelength. This wavelength is not near the peak of DNA absorption, and therefore contains less damaging potential than the UVC wavelength range. The distance from the sample to the light source was 2 cm. Mori et al. (2007) also conducted experiments to find the *E. coli* inactivation due to an LED emitting light at 405 nm and a low-pressure mercury lamp emitting light at 254 nm. Mori et al. found that a UVA fluence (365 nm) of 54 J/cm^2 resulted in a 3.9 log reduction of *E. coli* DH5α. For the *E. coli* irradiated by the LED at 405 nm, no inactivation was found. The experiment to compare irradiation using a low-pressure mercury lamp versus the 365 nm LED consists of placing microbial samples under each light source for 15 minute and 30 minute time exposures. For the 15-minute exposure time, the low-pressure mercury lamp induced a 2 log inactivation whereas the 365 nm LED induced less than a 0.5 log inactivation. However for the 30-minute exposure time, the LED induced a higher log inactivation of around 3.5, compared to around 3 for the low-pressure lamp (Mori et al., 2007). Unfortunately, Mori et al. (2007) did not report whether correction factors

recommended by Bolton and Linden (2003) were used as part of determining the UV fluence response curve for the UVA LEDs. Consequently, it is unknown whether the reported microbial inactivations were due to the incident or average UV fluence. If correction factors were used (i.e. water factor, Petri factor, etc.), then results could be more readily compared with standardized UV dose-response curves in the literature.

Vilhunen et al. (2009a) investigated the effect of UV irradiation from 269 and 276 nm UV-LEDs on another strain of *E. coli* (K12). The setup consisted of two batch reactors including ten LEDs in each. Each reactor had a viewing angle of 120^{o} and contained LEDs emitting light at either 269 or 276 nm. The UV-LEDs were attached with a clamp 1 cm above the microbial sample. The radiant fluxes from the 269 and 276 nm LED systems were measured as 5.8 and 11.6 mW, respectively. Results showed 3 to 4 log reductions within 5 minutes for experiments using both wavelengths. Also, despite the 276 nm system having a much higher radiant flux, the log inactivations due to both reactors for all exposure times were very similar. Therefore, it was concluded that irradiation by UV-LEDs at the wavelength 269 nm produced more efficient inactivation than that at 276 nm (Vilhunen et al., 2009a). Vilhunen et al.'s study was valuable to show wavelengths near the peak of DNA absorption may be more efficient than higher wavelengths still in the germicidal range even if the power output is much lower. Of the three studies mentioned that utilized UV-LEDs to inactivate microorganisms, only one reported the microbial inactivation in response to specific fluences. The other studies

only reported exposure times, which is not useful when comparing the results to UV fluence response curves in the literature utilizing other UV light sources.

Several studies that combined UV-LED irradiation and H_2O_2 for the degradation of phenol have also been completed. Vilhunen et al. (2009b) compared phenol degradation due to LEDs emitting wavelengths of 255, 265, and 280 nm with a viewing angle of 120^o. The highest and lowest quantum yields of phenol degradation were at 255 and 280 nm, respectively. It was suggested that the efficiency of the 255 nm reactor was due to low absorption of phenol and high absorption of H_2O_2, producing the largest amount of hydroxyl radicals (Vilhunen et al., 2009b). In Vilhunen et al. (2010), the reaction quantum efficiencies in response to wavelength and ratio of H_2O_2 to phenol were analyzed. Statistical tools were utilized to determine which parameters were most significant in phenol degradation. Batch reactors consisting of 10 LEDs were made for each wavelength (255, 269, and 276 nm) with optical powers of 0.31, 0.58, and 1.16 mW. As in the other study, as the wavelength increased, the quantum efficiency decreased. Also, higher ratios of H_2O_2 to phenol produced higher quantum efficiencies (Vilhunen et al., 2010). It was concluded that although the rate of phenol degradation was slower with UV-LEDs than with typical mercury lamps, the energy consumption was less. Also, as the deep UV-LED technology has not been optimized, results using the preliminary technology show potential for their use in water treatment applications (Vilhunen et al., 2010).

2.6 CHALLENGE MICROORGANISMS

In UV reactor validation, MS-2 coliphage is a commonly used surrogate for indicating viral response to UV irradiation. MS-2 is more resistant to UV disinfection than most human enteric viruses and is comparable in size and shape to many viruses (Bohrerova et al., 2006). The MS-2 UV fluence-response curve is represented by a log-linear function (Sommer et al., 1998). Recently, a detailed study was performed by Fallon et al. (2007) to explore alternative non-pathogenic microorganisms that can be used during the validation of continuous flow UV reactors. Fallon et al.'s study was performed since the current non-pathogenic surrogates (MS-2 and B. *subtilis*) were significantly more resistant than the target regulated pathogen (*Cryptosporidium*), resulting in a RED bias due to the difference in UV response kinetics, non-ideal reactor hydraulics, and non-uniform light distribution. As a result, the EPA UV Disinfection Guidance Manual (UVDGM) (EPA, 2006) has suggested the use of computing a RED bias factor to account for these issues. The goal of Fallon et al's study was to reduce one portion of the RED bias by matching the UV response kinetics between the challenge and target microorganisms.

Fallon et al. tested several bacteriophages and found two that had similar UV response to *Cryptosporidium* (T7 and SP8) and one that was in between *Cryptosporidium* and MS-2 (Qb). All three bacteriophages had limiting factors for use as a *Cryptosporidium* surrogate. For T7 and SP8, propagation resulted in low viral concentrations, making it difficult to reach necessary concentrations for validation testing

of larger volume reactors. Qb was found to be unstable in certain groundwaters, meaning that the concentration decreases with time. This instability over time severely limits Qb's potential for use during validation testing of a treatment plant because it is often impossible to plate all samples on the same day as the testing (Fallon et al., 2007). Reactors based on UV-LEDs will likely be low flow devices making it possible to utilize T7 as an appropriate surrogate that mimics *Cryptosporidium* UV response kinetics.

Although not commonly used in UV reactor validation, nonpathogenic strains of *E. coli* were used in this study due to low power outputs corresponding to UV-LEDs. *E. coli* is less resistant to UV disinfection than MS-2, allowing relatively efficient removal in the presence of lower UV fluence rates. Despite the low relevance of *E. coli* studies to drinking water treatment in the U.S., increased knowledge of the effect of UV-LED irradiation on *E. coli* may prove useful for potential UV-LED applications in developing countries.

2.7 UV-LED WAVELENGTHS

UV-LEDs in the germicidal range currently have low power outputs that are a function of the emitting wavelength and the current provided. For example, the maximum optical power output of a UVTOP UV-LED is around 0.5 mW at 260 nm and 0.75 mW at 280 nm for a current value of 30 mA (S-ET, Inc., 2008). The power output will decrease if a lower current is provided. The UV absorption curve for DNA (Figure 2.1) displays a peak around 260-265 nm, indicating this range as the most effective for

germicidal inactivation (Kalisvaart, 2004). However, the curve still displays significant absorption at higher wavelengths (e.g. 270-280 nm). In Linden et al. (2001), data indicated that UV exposure at wavelengths around 270 nm produced the greatest *Cryptosporidium parvum* inactivation. Mamane-Gravetz et al. (2005) determined the action spectra of MS2 and *B. subtilis*, or the relative efficiency of UV wavelengths at inactivating the two microorganisms. Figure 2.1 displays the relative spectral UV sensitivity coefficient of *B. subtilis* and MS-2 normalized relative to the sensitivity at 254 nm along with the DNA absorbance normalized to the DNA absorbance at 254 nm. Above 240 nm, the spectral sensitivity of MS-2 closely follows the DNA absorbance curve, showing a peak around 260 nm (Mamane-Gravetz et al., 2005). Gates (1929) determined that between 254 nm and 302 nm, the germicidal effectiveness of UV wavelengths for *E. coli* also closely matched the DNA absorbance spectra. Linden et al. (2001) suggested that the use of a UV source emitting between 240 and 280 nm is reasonable for water disinfection purposes. Therefore, it may be valuable to study if the higher LED power output at wavelengths larger than 260 nm compensates for the reduction in the germicidal efficiency. Due to the decrease in UV-LED efficiency at shorter wavelengths and the influence of light source power requirements in overall reactor power cost, it is important to assess the microbial inactivation at several wavelengths around the peak germicidal efficiency. This study utilized UV-LEDs emitting at 255 nm and 275 nm in order to determine whether the microbial UV dose response from UV-LEDs at 255 nm is similar to that of low-pressure mercury lamps

emitting at 254 nm and to study if the higher power output of 275 nm compensates for its lower germicidal effectiveness.

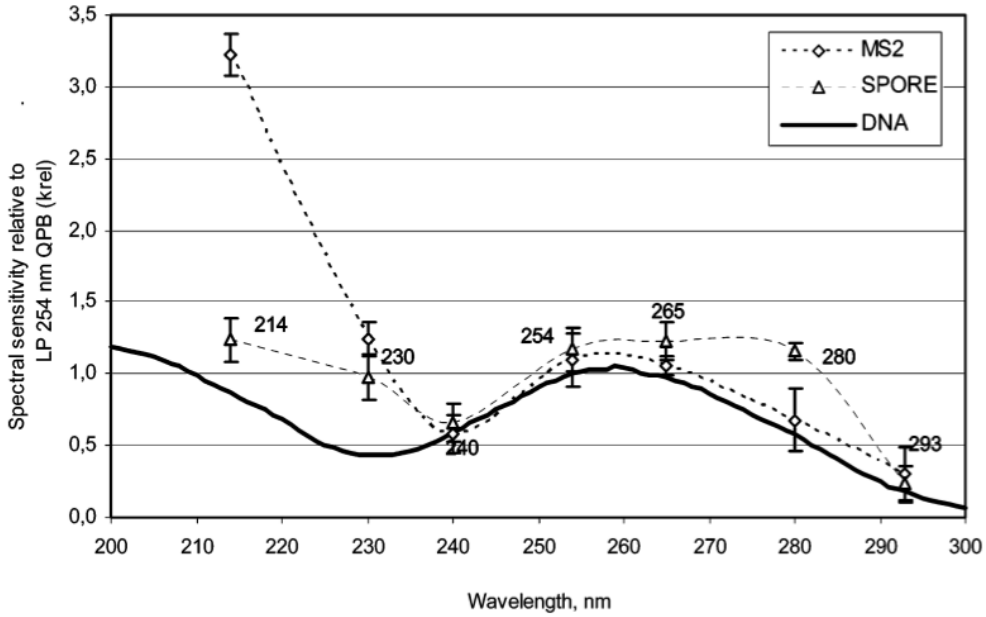

Figure 2.1. DNA Absorbance Spectrum (Mamane-Gravetz et al., 2005)

2.8 TIME DOSE RECIPROCITY

From a photochemical perspective, the damage caused by UV irradiation is only a function of the UV dose, given by the Bunsen-Roscoe reciprocity law where UV dose is equal to UV intensity multiplied by exposure time (Kalisvaart, 2004). However, the influence of biological processes such as repair enzymes may cause damage by UV irradiation to also be influenced by either the magnitude of the UV intensity or the exposure time even when the product leads to equivalent UV dose (Kalisvaart, 2004). Harm (1980) studied the influence of varying UV intensities and exposure times with

equal UV doses on the microbial inactivation of *E. coli*. It was determined that inactivation levels were significantly higher for shorter exposure times combined with higher UV intensities (Harm, 1980). Sommer et al. (1998) sought to determine the validity of time-dose reciprocity for UV irradiation by analyzing the UV dose response characteristics of several microorganisms (including MS2 and *E. coli*) when different UV intensities were used to achieve the same UV dose. It was found that all *E. coli* strains had a lower log reduction for the same UV fluence with a lower UV intensity for fluences between 80 and 100 J/m^2. These results suggest that for *E. coli*, a higher UV intensity combined with a lower exposure time is more effective than a lower UV intensity with a higher exposure time. Similar results were found in Harm (1980). Sommer et al. (1998) hypothesized that higher inactivation levels resulting from high UV intensities combined with low exposure times may have been due to the cell repair enzymes being more susceptible to high UV intensities. All other studied microorganisms (including MS2) produced no change in fluence response between high and low UV intensity experiments (Sommer et al., 1998).

2.9 FLUENCE RATE MODELS

Liu et al. (2004) performed a study that compared seven fluence rate models with measurements from actinometer experiments performed in air and water. In Liu et al. (2004), the models compared were the line source integration (LSI), multiple points source summation (MPSS), multiple segment source summation (MSSS), UVCalc3D,

RAD-LSI, view factor, and radiative transfer equation using the discrete ordinate (DO) approach. Descriptions of these models are provided in Table 2.1 (Lui et al., 2004):

Table 2.1. Descriptions of Fluence Rate Models

Model	Description
MPSS	• Assumes a linear lamp emission is equal to the emission of a certain number (n) of point sources spaced equally along the lamp axis • Assumes each point source outputs a power P/n where P is the total UV power output of the lamp • Considers refraction, reflection, and absorption • Modeling cylindrical lamp as point sources causes an overprediction in fluence rate distribution near the lamp surface and an inaccurate fluence rate profile along the lamp length
MSSS	• Similar to MPSS by including refraction, reflection, and absorption • Corrects for MPSS overprediction, modeling the lamp as a series of cylindrical segments • Produces a more accurate light emission profile along the lamp length
UV Calc 3D	• Similar to MSSS but applies a factor to account for the quartz sleeve
LSI	• The continuous (integral) form of MPSS • Efficient method compared to the MPSS due to its closed-form solution • A limit is that the closed-form solution only exists when absorption, reflection, and refraction are not included • Has been shown to be effective only for fluence rate distribution prediction far away from the lamp

Table 2.1. Continued

Model	Description
RAD-LSI	• Accounts for the radial direction of the light emission closer to the lamp surface by including a model for the radial intensity calculation into the LSI
View Factor	• Calculates irradiance for a differential element in space due to a cylindrical surface • Predicts the radiation fraction that hits the differential element from the surface of the lamp section • Can account for absorption, reflection, and refraction
DO	• A numerical method for solving the radiative transfer equation • Accounts for radiation in an absorbing medium • The version of DO used in this study did not include light refraction

Some conclusions from this study include (Liu et al., 2004):

- RAD-LSI provided better performance than LSI near the lamp
- MSSS and UVCalc3D produced similar results, indicating that the quartz sleeve can be approximated by the factor used in UVCalc3D
- Similar fluence rate distributions were predicted by RAD-LSI and view factor near the lamp surface, but RAD-LSI predicted lower fluence rates further away from the lamp

- DO over-predicted near the lamp surface and under predicted far from the lamp surface

Although MPSS was not recommended as the best performer in Liu et al.'s (2004) study, it was used in this study to predict the UV-LED output in a collimated beam apparatus. It is likely that the MPSS will best predict UV-LED output as they are small point sources. Therefore, the over prediction that occurs when modeling a cylindrical mercury lamp as a number of point sources may not be present when modeling UV-LED light output.

3. METHODS

3.1 UV-LED COLLIMATED BEAM DESIGN

Collimated beam experiments were performed with UV-LEDs to determine the UV response kinetics of the challenge microorganisms (MS-2, T7, and *E. coli*). UV-LEDs were obtained from Sensor Electronic Technologies in Columbia, SC. Experimental tests were performed with LEDs emitting two unique wavelengths (255 and 275 nm). The two wavelengths represent LEDs with significant differences in power efficiencies that would impact the UV response kinetics of the microorganisms.

Comsol Multiphysics, a numerical modeling and CFD software (Comsol Inc., Burlington, MA) was utilized to design an optimal collimated beam apparatus configuration with design parameters including the number of UV-LEDs, length of collimator tube, and height of samples relative to light source. The incident fluence rates

on a microbial sample in the UV-LED collimated beam apparatus were predicted using a simple point source summation model (Bolton, 2000). In a collimated beam apparatus, irradiance is equivalent to fluence rate. As the objective of the model was to find the incident irradiance on the sample, transmittance and absorbance of the sample was not included in model simulations. In this case, the irradiance for a non-absorbing medium at a distance r from the point source can be described by Equation 3.1 (Bolton, 2000):

$$I = \frac{P}{4\pi r^2} \tag{3.1}$$

where I = irradiance and P = radiant power from the light source

However, the UVTOP UV-LEDs used in this study have a 60^{o} viewing angle (Figure 3.1), meaning that the power is only distributed over a certain fraction of the surrounding spherical surface area from the point source.

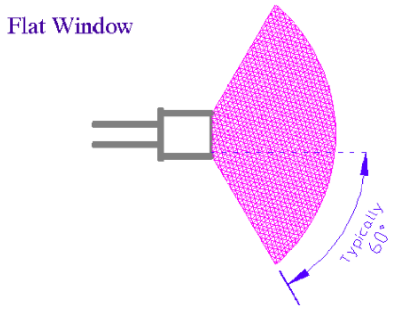

Figure 3.1. Viewing Angle for UVTOP UV-LED (S-ET, Inc.)

This narrow distribution of power was corrected in the irradiance calculation for each UV-LED assuming all the power was projected onto a spherical cap at a distance r from the UV-LED shown in Equation 3.2:

$$I = \frac{P}{2\pi r^2 (1 - \cos\alpha)} \tag{3.2}$$

where α is 60 degrees. The model assumes that irradiance values are zero outside the viewing angle. The total incident irradiance at each point on the sample surface is equal to the sum of the irradiances from the individual LEDs. In order to determine the optimal LED configuration for both sets of wavelengths, several spatial arrangements for each set were analyzed. Figure 3.2 and Figure 3.3 display examples of simulated arrangements explored in this study. The 255 and 275 nm LED arrays consisted of 8 LEDs and 4 LEDs respectively because the power output of 275 nm LEDs was over double that of the 255 nm LEDs. For each arrangement, the light intensity distribution over the plane representing the sample surface area was analyzed for a range of distances from the light source. The Petri Factor and the average irradiance values were used to determine the optimal configuration for each LED wavelength setup. An ideal configuration would allow a Petri Factor of approximately 0.9 while still maintaining a high irradiance value to achieve reasonable exposure times for a desired UV dose.

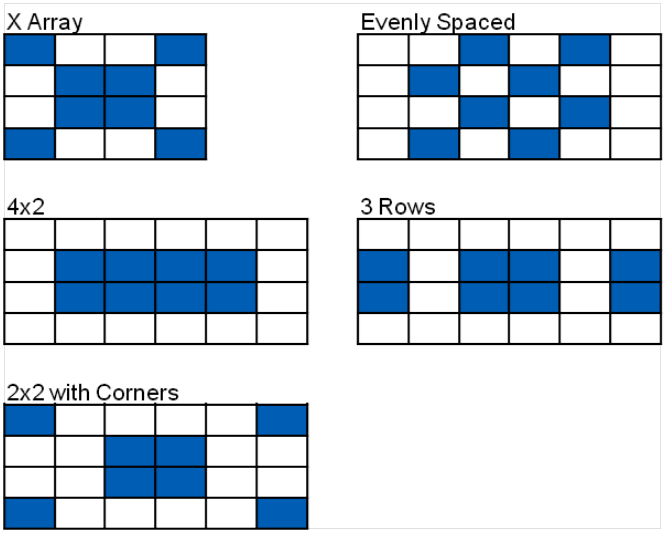

Figure 3.2. Spatial Arrangements for 255 nm UV-LEDs (Set of 8 LEDs)

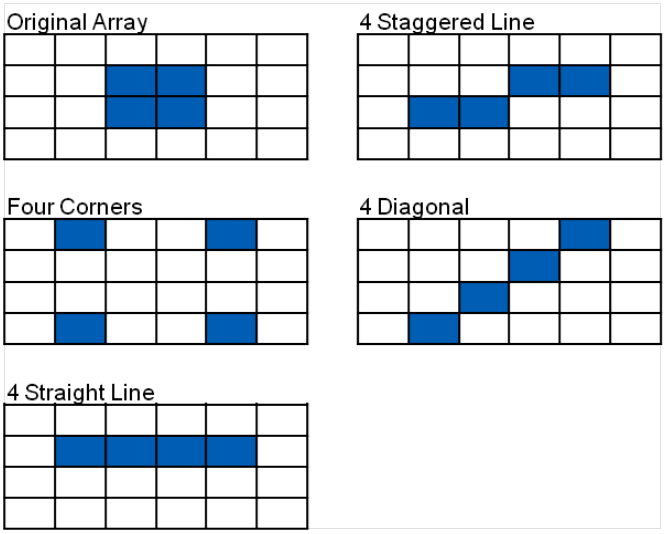

Figure 3.3. Spatial Arrangements for 275 nm UV-LEDs (Set of 4 LEDs)

The collimated beam apparatus was constructed to allow for the UV-LEDs at 255 nm and 275 nm and their electrical equipment to be interchangeable. The manufacturer of the UV-LEDs (SET, Inc.) recommended 20mA and a maximum of 200mA to be used.

Above this current value, more heat is dissipated than the amount of the UV light. Resistors in series were used to limit this current flow to each UV-LED. Pairs of UV-LED and resistor were connected in parallel to the DC power source Agilent 6614C. The current set in the power source is 20mA multiplied by the number of LEDs.

The apparatus consisted of a 56 cm x 56 cm box with the LEDs centered at the top in either a 4x2 or 2x2 array. The array configurations were based on the Comsol simulations that will be discussed in the results section.. Both arrays of LEDs were contained within a 7.6 cm x 7.6 cm metal holder that allowed for heat dissipation. A thin metal shutter was located directly below the LEDs to ensure accurate exposure times. Inside the box was a platform and stir plate that could be raised to make the sample surface as close as 3.3 cm away from the LEDs. The collimating tube was approximately 3.3 cm long with a diameter of 10.2 cm. Figure 3.4 displays the front and top view of the UV-LED Collimated Beam Apparatus.

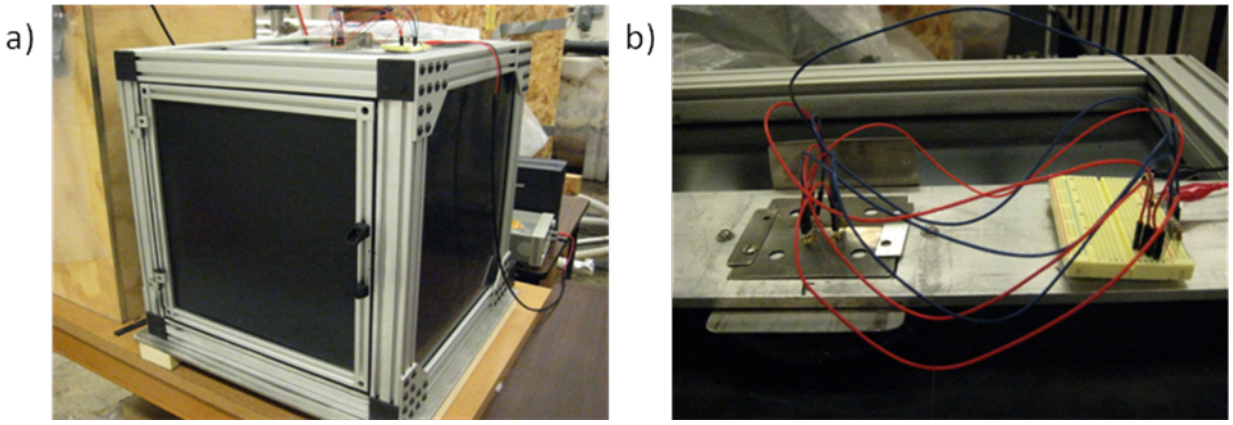

Figure 3.4. Front and Top View of the UV-LED Collimated Beam Apparatus

3.2 UV-LED COLLIMATED BEAM EXPERIMENTS

50 mm x 30 mm glass Petri dishes holding micro stir bars were placed under a low-pressure mercury lamp prior to experiments to inactivate any background microorganisms in the dishes. After the appropriate stock solution was diluted and split into evenly mixed 10 mL samples, the absorbance was found with a HACH DR 5000 Spectrophotometer at the wavelength corresponding to the UV-LED or low-pressure mercury lamp wavelength output (depending on which light source was being used for the experiments). The absorbance corresponding to the wavelength of the UV light source was used to find the water factor as described in Bolton and Linden (2003). For the UV-LED experiments, a Stellarnet EPP2000C-100 Spectrometer with an attached fiber optic probe to capture fine planar variations in light intensity was calibrated at both 255 and 275 nm and used to find the Petri factor as described in Bolton and Linden (2003) for all experiments. Outputs from the Stellarnet EPP2000C Spectrometer show that the UV-LEDs in this study actually emit at a small range of wavelengths, with the majority at the peak value of either 255 nm or 275 nm, as shown in Figure 3.5 and Figure 3.6. The absorbance was also taken at the maximum and minimum wavelengths emitted by each UV-LED and the difference in absorbance from peak wavelength to the outside range was negligible.

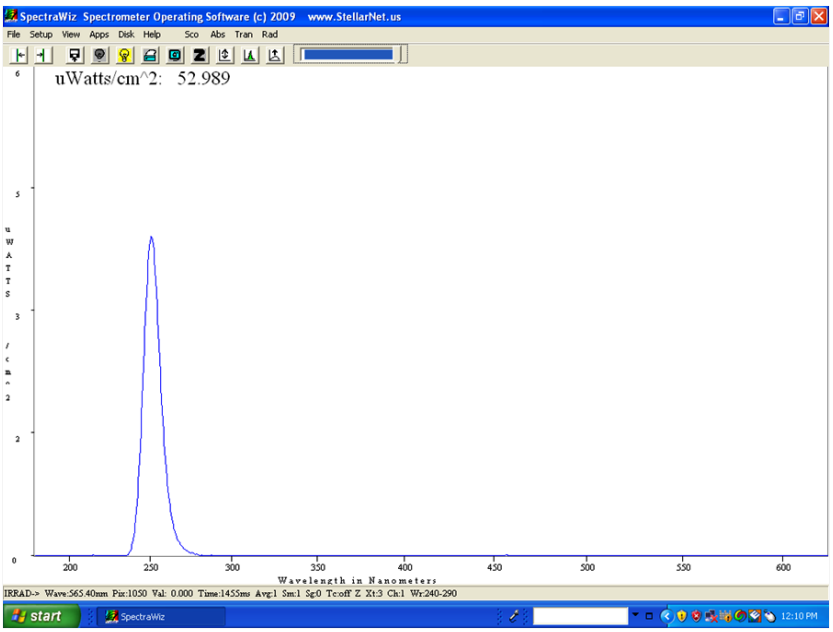

Figure 3.5. 255 nm LED Output from Stellarnet Spectrometer

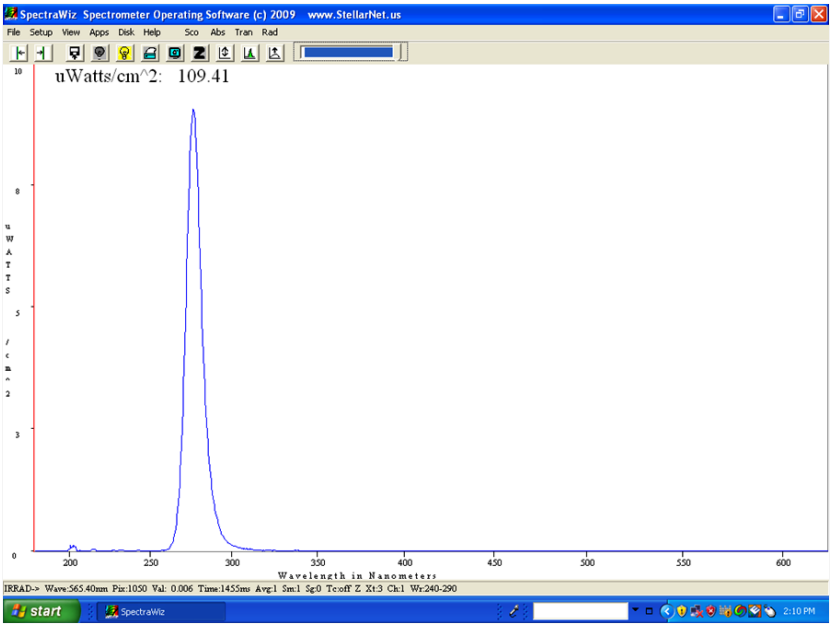

Figure 3.6. 275 nm LED Output from Stellarnet Spectrometer

For the low-pressure mercury lamp experiments, a UVX Digital radiometer (UVP, Inc.) was used to find the incident irradiance and Petri factor. Both radiometers were checked with a potassium iodide actinometry method (Rahn, 1997; Rahn, 2003) (Appendix C). The required incident fluence for each desired average fluence was then calculated using Equation 3.3 where the incident fluence is the exposure time multiplied by the center irradiance value found with the radiometer.

$$I_{avg} = I_{incident} \times \text{Petri Factor} \times \text{Reflection Factor} \times \text{Water Factor} \times \text{Divergence Factor} \quad (3.3)$$

The range of average doses paralleled the UV dose ranges in Sommer et al. (1998) and Bohrerova et al. (2008), which contain the dose-response curve for MS-2, *E. coli,* and *T7* irradiated by a UV low-pressure mercury lamp (0-60 mJ/cm^2 for MS2, 0-20 mJ/cm^2 for T7, and 0-12 mJ/cm^2 for *E. coli*). Table 3.1 displays the incident irradiance and exposure time ranges for each microorganism.

Table 3.1. Irradiance and Exposure Time Ranges

	Incident Irradiance Range (mW/cm^2)			Exposure time range (sec)		
	LP	275	255	LP	275	255
T7	0.32-0.33	0.090-0.10	0.048-0.057	0-50	0-310	0-634
MS2	0.32	0.089-0.10	0.046-0.057	0-164	0-859	0-1577
E. coli	0.34	0.094-0.11	0.049-0.060	0-33	0-158	0-292

Care was taken to place the top of the sample level at the same distance from the UV source as the radiometer sensor during measurements. After irradiation was complete for

each sample, a sterile syringe was used to place the sample in a sterile 15 mL centrifuge tube to prevent contamination.

3.3 MICROORGANISMS

Bacteriophages

MS-2 coliphage (ATCC 15597-B1) and T7 coliphage received from Clancy Environmental Consultants were propagated and enumerated according to the methods described in Bohrerova, 2006 and Bohrerova, 2008, respectively. The bacteriophages were kept in a 4 ^{o}C refrigerator and put on ice when used during experiments.

Escherichia coli Host Preparation

An inoculating loop was sterilized by flaming and allowed to cool. Using the loop, a small amount of the corresponding stock *E. coli* (Table 1) was scraped off the top without allowing the stock to thaw, placed on tryptone bottom agar (Appendix B), and put in a 37 ^{o}C incubator overnight. In the morning, the appropriate broth (Table 1) was inoculated with the overnight culture and placed in an incubator shaker at 37 ^{o}C for 4-6 hours. The volume of broth was a function of the number of plates being used for the experiment; making sure to have at least 1 mL broth per agar plate.

Bacteriophage Enumeration

A small volume of stock phage solution was diluted in the appropriate sterile solution (Table 3.2) in 45 mL centrifuge tubes and shaken to ensure consistent concentrations for all irradiated samples. MS-2 and T7 are temperature sensitive, so all samples were kept on ice with the exception of the irradiation experiments. After irradiation experiments, serial dilutions of 0.1 mL phage sample in 0.9 mL of sterile solution were completed for each sample based on the dilution determined necessary for plates to contain plaque counts between 20 and 200. Before the phage dilutions were completed, tryptone top agar (Appendix B) was prepared and autoclaved so the agar would be able to cool in a water bath placed at 45 ^{o}C by the time the serial dilutions were completed. Tryptone bottom agar plates that had been warmed in a 37 ^{o}C incubator for at least one hour were placed in the sterile laminar flow fume hood and labeled based on the sample fluence and dilution. Phage samples and *E. coli* broth incubated for 4-6 hours in a 37 ^{o}C incubator shaker were brought next to the water bath to allow samples to be added while agar was being warmed. When the *E. coli* broth was not being used, it was kept in a 37 ^{o}C incubator. Four mL aliquots of tryptone top agar were added to 15 mL centrifuge tubes in series of 12. *E. coli* broth was added in 1 mL volumes to the tubes in series of 6 to minimize a length exposure of *E. coli* to 45 ^{o}C. *E. coli* and MS-2 should not be warmed at 45 ^{o}C longer than 15 minutes and 1 minute, respectively (Malley et al., 2004). The phage sample was vortexed and 0.1 mL was added to a centrifuge tube containing agar and the *E. coli* host. The tube was then inverted twice to mix the contents and

poured over the appropriately labeled bottom agar plate. The plate was gently swirled to allow agar to cover the entire plate. Agar was allowed to harden and incubated in the inverted position at 37 ^{o}C for 18-24 hours for MS-2 and 5 hours for T7. After incubation, plates that contained 20-200 plaques were counted.

Bacteriophage Stock Solution

Once a month or when the MS-2 stock solution concentration decreased sufficiently, MS-2 was propagated to make new stocks. T7 is more stable, allowing new stocks to be prepared less frequently than MS-2. Petri dishes were inoculated with MS-2 or T7 stock as described in the bacteriophage enumeration section and incubated in the inverted position at 37 ^{o}C for 24 hours or 5 hours, respectively. After incubation, 5 mL of sterile saline-calcium solution was added to all plates and left to sit for 30 minutes. Each plate was then poured through a sterile funnel into a plastic centrifuge tube. Sterile pipettes were used to put equal volumes into an even number of glass centrifuge tubes, which were centrifuged for 15 minutes at 5,000 rpm and 4 ^{o}C. The supernatant was filtered through a 0.2 um cellulose acetate membrane syringe filter and stored in 45 mL light sensitive centrifuge tubes at 4 ^{o}C.

Table 3.2. Microorganism Specifications

Microorganism	E. coli Host	Broth*	Agar*	Solution*
MS-2 (15597-B1)	ATCC 15597	tryptone	tryptone	saline-calcium
T7	ATCC 11303	TSB and 0.5% NaCl	tryptone	PBS
E. coli (11229)	N/A	nutrient	nutrient	PBS

*Appendix B for broth, agar, and solution preparations

Escherichia coli Stocks

A loop of *E. coli* from frozen stock was added into the appropriate broth or striked onto the appropriate agar (Table 3.2) and incubated at 37 ^{o}C overnight. A loop of overnight culture was added to 10 mL of fresh broth and put in an incubator shaker at 37 ^{o}C for 3-4 hours to achieve a semi-log growth phase. Aliquots of *E. coli* broth (0.5 mL) were added to 0.5 mL of 10% glycerol in small sterile centrifuge tubes. These tubes were then vortexed and placed in -20 ^{o}C for storage.

Escherichia coli 11229

A volume of 0.2 mL *E. coli* (ATCC 11229) stock was added to 50 mL nutrient broth and placed in an incubator shaker at 37 ^{o}C for 18-24 hours. After a stock tube was used, it was discarded due to the reduction in viability of *E. coli* stocks after thawing. Following incubation, 10 mL of broth was added to two sterile centrifuge tubes and centrifuged at 5,000 rpm for 5 minutes. Unlike the bacteriophages, *E. coli* 11229 was

kept at room temperature throughout experiments and during centrifugation. The liquid in both tubes was then poured out, 10 mL of sterile PBS was subsequently added to the tube and the tube was shaken. The process of centrifugation and washing with PBS was repeated and 1 mL of the resulting solution was diluted in 45 mL PBS to produce a concentration of approximately $1x10^8$ cfu/mL for irradiation experiments. After irradiation, serial dilutions of 0.1 mL *E. coli* sample in 0.9 mL of sterile PBS were completed for each sample based on the dilution that was assumed necessary for plates to contain counts between 20 and 200. The necessary dilutions were then spread on warmed nutrient agar plates in 0.1 mL volumes. The plates were incubated upside down at 37 ^oC for 18-24 hours and plates yielding 20 to 200 cfu were counted.

4. JOURNAL ARTICLE

Title: Microbial UV Fluence-Response Assessment using a Novel UV-LED Collimated Beam System

Authors:

(1) Colleen Bowker, MS
Department of Civil, Construction, and Environmental Engineering
North Carolina State University
Mann Hall, Box 7908
Raleigh, North Carolina 27695
Phone: 704-906-2749 Email: ckbowker@gmail.com

(2) Amanda Sain
Undergraduate Research Assistant
Department of Civil, Construction, and Environmental Engineering
North Carolina State University
Mann Hall, Box 7908
Raleigh, North Carolina 27695
Phone: 980-621-8620 Email: sainae@gmail.com

(3) Max Shatalov
1195 Atlas Road
Columbia, SC 29209
Phone: 803-647-9757 Fax: 803-647-9770

(4) Joel Ducoste, PhD
Professor
Civil, Construction and Environmental Engineering
North Carolina State University
Mann Hall 319c, Box 7908
Raleigh, North Carolina 27695
Phone: 919-515-8150 Fax: 919-515-7908 Email: jducoste@eos.ncsu.edu

ABSTRACT

The use of ultraviolet (UV) light for disinfection applications has become increasingly popular due to the ability of UV to inactivate chlorine resistant microorganisms and disinfect without the production of known disinfection by-products. The most widely used UV light sources are low- and medium-pressure mercury lamps. Technology that has recently become available is UV light emitting diodes (UV-LEDs) with emission wavelengths in the germicidal range. UV-LEDs do not contain toxic mercury, offer design flexibility due to their small size, and have a longer operational life than mercury lamps. This research sought to determine the UV fluence-response of several target non-pathogenic microorganisms to UV-LEDs by performing collimated beam tests. Comsol Multiphysics was utilized to create an optimal UV-LED collimated beam design based on number and spacing of UV-LEDs and distance of the sample from the light source while minimizing the overall cost. The optimized UV-LED collimated beam apparatus and a low-pressure mercury lamp collimated beam apparatus were used to determine the UV fluence-response of three surrogate microorganisms (*E. coli*, MS-2, *T7*) to 255 nm UV-LEDs, 275 nm UV-LEDs, and 254 nm low-pressure mercury lamps. Irradiation by low-pressure mercury lamps produced greater *E. coli* and MS-2 inactivation than 255 nm and 275 nm UV-LEDs and similar T7 inactivation to irradiation by 275 nm UV-LEDs. The 275 nm UV-LEDs produced more efficient T7 and *E. coli* inactivation than 255 nm UV-LEDs while both 255 nm and 275 nm UV-LEDs produced comparable microbial inactivation for MS-2. Differences may have been caused by a departure from the time-dose reciprocity law due to microbial repair mechanisms.

4.1 INTRODUCTION

The use of ultraviolet (UV) light in drinking water disinfection applications has become a growing alternative to chemical disinfectants since its determination as an effective method for inactivating chlorine resistant pathogenic organisms without the production of any known disinfection by-products (Bohrerova et al., 2006). The majority of UV disinfection systems currently use low- or medium-pressure mercury lamps, which are toxic, require significant amounts of energy, and have a short lifetime. Other alternative UV light emission sources have been developed (Wang et al., 2005; Bohrerova et al., 2008). A possible alternative to UV mercury lamps or these alternative UV emission sources for point of use applications is the use of UV light emitting diodes (UV-LEDs). UV-LEDs contain no known toxic elements that can be released upon breakage and have a much longer lifetime. In addition, UV-LEDs provide design flexibility due to their small size (Shur and Gaska, 2008). Recent advances in technology have allowed the production of UV-LEDs with emission wavelengths in the germicidal range, with the shortest wavelength at 237 nm (Shur and Gaska, 2008).

Light-emitting diodes (LEDs) are created by connecting p-type and n-type semiconductors that move electrons into positively charged holes between these two materials. Light is generated when the electrons and holes collide at a junction. The wavelength of light will depend on the type of material used for the two semiconductors (i.e., indium gallium nitride for light in the visible range and aluminium gallium nitride and aluminium nitride for ultraviolet light) (Dume, 2006).

Recently, deep UV-LEDs with peak emission wavelength from 250 to 340 nm have been manufactured for many potential applications including microbial disinfection (Shur and Gaska, 2008). While mercury lamps only emit light at one wavelength, UV-LEDs are capable of emitting light at multiple wavelengths. Therefore, UV-LEDs are able to emit light at the exact peak of germicidal effectiveness for a particular organism (Shur and Gaska, 2008).

Several studies have analyzed the microbial response of different strains of *E. coli* to UV-LED irradiation. These studies suggested that UV-LEDs may inactivate microorganisms efficiently only over long exposure times (Crawford et al., 2005; Mori et al., 2007; Vilhunen et al., 2009). The long exposure times required in these studies were likely due to low power outputs from the UV-LEDs. UV-LED power inefficiency was listed as a constraint for UV-LED applicability in Shur and Gaska (2008), but it was also mentioned that efficiency may soon be improved by an order of magnitude or more since the technology is still in its infancy. An issue with the previously mentioned studies using UV-LEDs for microbial inactivation was that they did not use a standardized measurement of UV fluence delivered to the microorganisms; making the results difficult to compare to UV fluence response studies in the literature for low- or medium- pressure mercury lamp systems. In order to determine the UV fluence-response of different microorganisms to UV-LEDs comparable to those in the literature for low- and medium-pressure mercury lamps, it is necessary to build a UV-LED collimated beam apparatus based on the parameters listed in Bolton and Linden (2003) and use standardized

correction factors during irradiation experiments.

UV-LEDs in the germicidal range currently have low power outputs that are a function of the emitting wavelength and the current provided. For example, the maximum optical power output of a UVTOP UV-LED is around 0.5 mW at 260 nm and 0.75 mW at 280 nm for a current value of 30 mA (S-ET, Inc., 2008). The power output will decrease if a lower current value is provided.

The UV absorption curve for DNA displays a peak around 260-265 nm, indicating this range as the most effective for germicidal inactivation (Kalisvaart, 2004). However, the DNA UV absorption curve still displays significant absorption at higher wavelengths (e.g. 270-280 nm). Linden et al. (2001) suggested that the use of a UV source emitting between 240 and 280 nm is reasonable for water disinfection purposes. Therefore, it may be valuable to study if the higher UV-LED power output at wavelengths larger than 260 nm compensates for the reduction in the germicidal efficiency.

The objective of this study was to determine the UV dose-response of target non-pathogenic microorganisms to germicidal UV-LEDs by performing detailed collimated beam tests on MS-2 coliphage (commonly used surrogate for *Cryptosporidium* in biodosimetry tests), T7 coliphage (possible alternative surrogate that mimics *Cryptosporidium* UV response kinetics (Fallon et al., 2007)), and *E. coli*, which has a lower resistance to UV irradiation than the other two study microorganisms. The

collimated beam tests were completed using low-pressure mercury lamps and UV-LEDs with emissions at 255 nm and 275 nm to determine whether the microbial UV dose-response from UV-LEDs at 255 nm is similar to that of low-pressure mercury lamps emitting at 254 nm and to study if the higher power output of 275 nm compensates for its lower germicidal effectiveness.

4.2 METHODS

UV-LED Collimated Beam Design

Collimated beam experiments were performed with UV-LEDs to determine the UV response kinetics of the challenge microorganisms (MS-2, T7, and *E. coli*). UV-LEDs were obtained from Sensor Electronic Technologies in Columbia, SC. Experimental tests were performed with LEDs emitting two unique wavelengths (255 and 275 nm). The two wavelengths represent LEDs with significant differences in power outputs that may impact the UV response kinetics of the microorganisms. For a manufacturer recommended current value of 20 mA, the 255 nm and 275 nm UVTOP UV-LEDs produce a power output of approximately 0.3 mW and 0.5 mW, respectively.

Comsol Multiphysics, a numerical modeling and CFD software (Comsol Inc., Burlington, MA) was utilized to find an optimal collimated beam apparatus design with design parameters including the number of UV-LEDs, length of collimator tube, and height of samples relative to the light source. The incident fluence rates on a microbial sample in the UV-LED collimated beam apparatus were predicted using a simple point source summation model (Bolton, 2000). In a collimated beam apparatus, the irradiance

is equivalent to fluence rate. As the objective of the model was to find the incident irradiance on the sample, transmittance and absorbance of the sample was not included in model simulations. In this case, the irradiance over a surrounding spherical surface area for a non-absorbing medium at a distance r from the point source can be described by Equation 4.1 (Bolton, 2000):

$$I = \frac{P}{4\pi r^2} \tag{4.1}$$

where I = irradiance and P = radiant power from the light source

However, the UVTOP UV-LEDs used in this study have a 60^{o} viewing angle (Figure 4.1), meaning that the power from the point source is only distributed over a certain fraction of the surrounding spherical surface area.

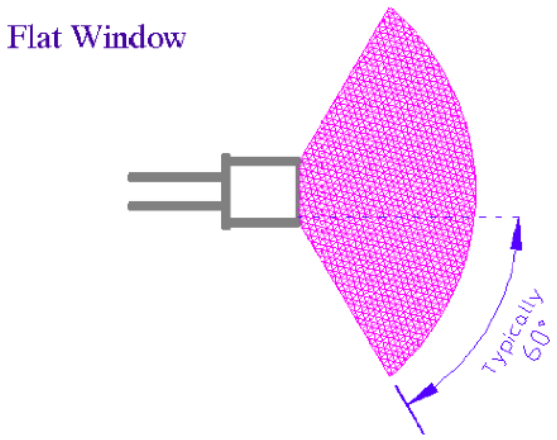

Figure 4.1. Viewing Angle for UVTOP UV-LED (S-ET, Inc.)

This narrow distribution of power was corrected in the irradiance calculation assuming all the power was projected onto a spherical cap at a distance r from the UV-LED shown in Equation 4.2:

$$I = \frac{P}{2\pi r^2(1-\cos(\alpha))} \tag{4.2}$$

where α is 60 degrees. The total incident irradiance at each point on the sample surface is equal to the sum of the irradiances from all individual LEDs, given by the distance r from each LED and Equation 4.2. In order to determine the optimal LED configuration for both sets of wavelengths, several spatial arrangements for each set were analyzed. Figure 4.2 and Figure 4.3 display examples of simulated arrangements explored in this study. The 255 and 275 nm LED arrays consisted of 8 LEDs and 4 LEDs respectively because the power output of 275 nm LEDs was over double that of the 255 nm LEDs. For each arrangement, the light intensity distribution over the plane representing the sample surface area was analyzed for a range of distances from the light source. The Petri Factor and the average irradiance values were used to determine the optimal configuration for each LED wavelength setup. An ideal configuration would allow a Petri Factor of approximately 0.9 (Bolton and Linden, 2003) while still maintaining a high enough irradiance to have reasonable exposure times for a desired UV dose.

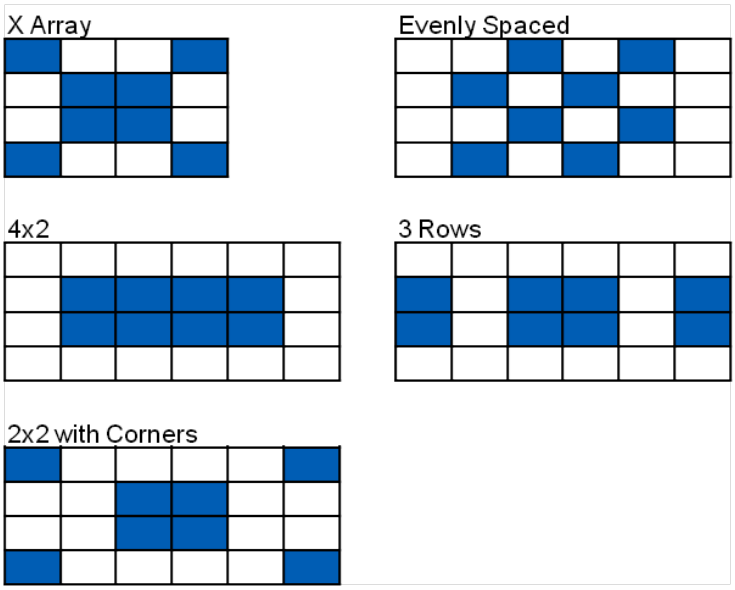

Figure 4.2. Spatial Arrangements for 255 nm UV-LEDs (Set of 8 LEDs)

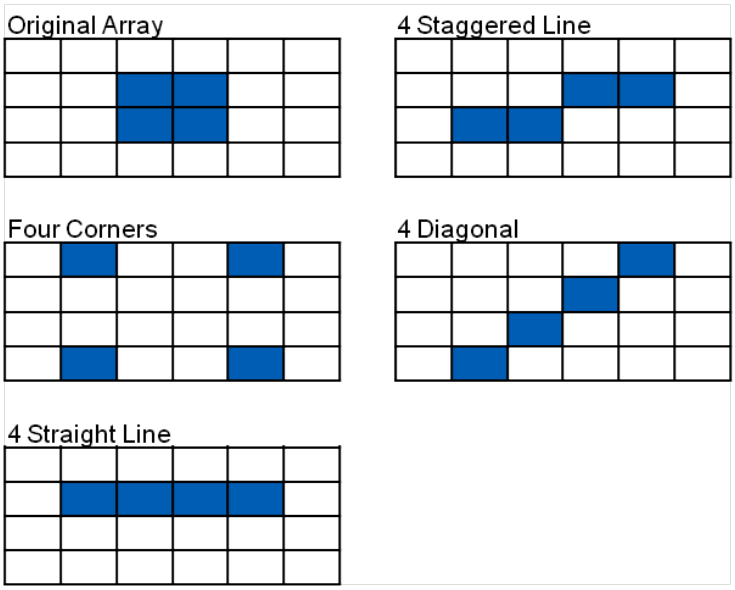

Figure 4.3. Spatial Arrangements for 275 nm UV-LEDs (Set of 4 LEDs)

A collimated beam apparatus was constructed to allow for the UV-LEDs at 255 nm and 275 nm and their electrical equipment to be interchangeable. A resistance in series was used to limit this current flow for each UV-LED. Pairs of UV-LED and resistor were connected in parallel to the DC power source. The apparatus consisted of a 56 cm x 56 cm box with the LEDs centered at the top in either an X configuration or 2x2 array. The array configurations were based on the Comsol simulations that will be discussed in the results section. Both arrays of LEDs were placed in a 7.6 cm x 7.6 cm metal holder that allowed for heat dissipation. The collimating tube was approximately 3.3 cm long with a diameter of 10.2 cm. Figure 4.4 displays the front and top view of the UV-LED Collimated Beam Apparatus.

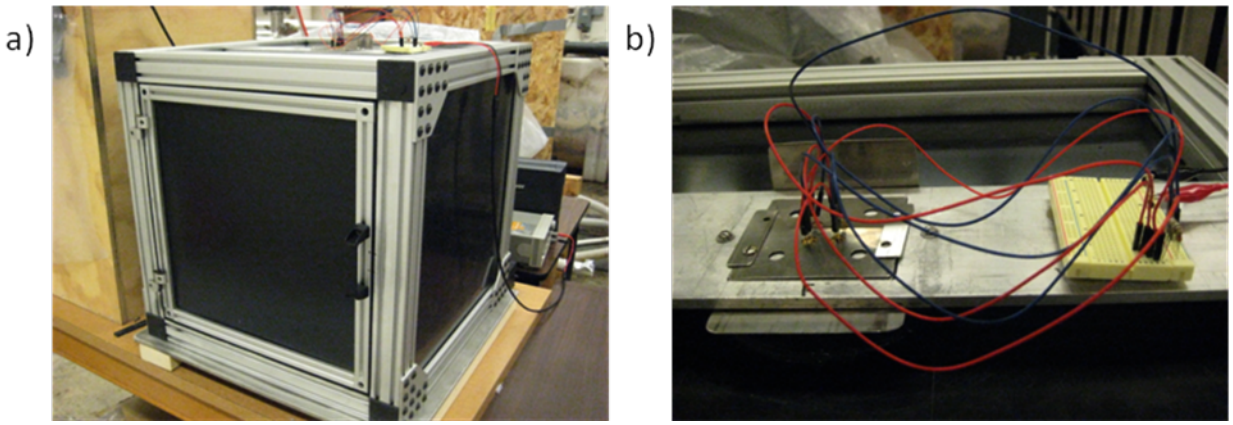

Figure 4.4. Front and Top View of UV-LED Collimated Beam Apparatus

UV-LED Collimated Beam Experiments

Bench scale experiments were completed using a collimated beam apparatus with either low-pressure mercury lamps (254 nm output), 255 nm UV-LEDs, or 275 nm UV-LEDs as the light source to determine the UV response kinetics of MS-2, T7, and *E. coli*. The absorbance of samples prior to irradiation was found with a HACH DR 5000 Spectrophotometer at the wavelength corresponding to the UV-LED or low-pressure mercury lamp wavelength output (depending on the light source used for the particular experiment) in order to determine the water factor (Bolton and Linden, 2003). The UV-LEDs used in this study emit at a small range of wavelengths, with the majority at the peak value of either 255 nm or 275 nm. The absorbance was also taken at the maximum and minimum wavelengths emitted by each UV-LED and the difference in absorbance from peak wavelength to the outside range was negligible. The protocol described for low-pressure mercury lamps in Bolton and Linden (2003) was used to find the average irradiance for the UV-LED and low-pressure mercury lamp experiments. The incident irradiance at the surface of the liquid sample was found for the UV-LED experiments using a Stellarnet EPP2000C-100 Spectroradiometer with an attached fiber optic probe to capture fine planar variations in light intensity calibrated at both 255 and 275 nm. For the low-pressure mercury lamp experiments, a UVX Digital radiometer (UVP, Inc.) calibrated at 254 nm was used to find the incident irradiance. Both radiometers were checked with a potassium iodide actinometry method (Rahn, 1997; Rahn, 2003).

The average UV fluence was calculated as the exposure time multiplied by the average irradiance. The range of average UV fluences paralleled the UV fluence ranges in Sommer et al. (1998) and Bohrerova et al. (2008), which contain the UV dose-response curve for MS-2, *E. coli,* and *T7* irradiated by a UV low-pressure mercury lamp (0-60 mJ/cm^2 for MS2, 0-20 mJ/cm^2 for T7, and 0-12 mJ/cm^2 for *E. coli*). Table 4.1 displays the incident irradiance and exposure time ranges for each microorganism.

Table 4.1. Irradiance and Exposure Time Ranges

	Incident Irradiance Range (mW/cm^2)			Exposure time range (sec)		
	LP	275	255	LP	275	255
T7	0.32-0.33	0.090-0.10	0.048-0.057	0-50	0-310	0-634
MS2	0.32	0.089-0.10	0.046-0.057	0-164	0-859	0-1577
E. coli	0.34	0.094-0.11	0.049-0.060	0-33	0-158	0-292

Microorganisms

MS-2 coliphage (ATCC 15597-B1) and T7 coliphage received from Clancy Environmental Consultants were propagated and enumerated according to the methods described in Bohrerova, 2006 and Bohrerova, 2008, respectively. For enumeration, the appropriate *E. coli* host (Table 4.2) was cultivated using the appropriate broth (Table 4.2) in an incubator shaker at 37 ^oC for 4-6 hours. Tryptone-based top agar was placed in 4 mL centrifuge tubes in a water bath at 45 ^oC. 1 mL of *E. coli* host and 0.1 mL of the appropriate bacteriophage (MS-2 or T7) dilution were added to a 4 mL centrifuge tube of top agar and poured onto tryptone-based bottom agar. Samples were plated in triplicate. After the agar solidified, plates were incubated at 37 ^oC in the inverted position for 18-24

hours for MS-2 or 5 hours for T7. Plates that contained between 20 and 200 plaques were counted. The method was similar for propagation, except for after incubation, where 5 mL of the appropriate sterile solution (Table 4.2) was poured onto the plates and left to sit for 30 minutes. The top agar was then scraped off the plates and centrifuged for 15 minutes at 5,000 rpm and 4 ^{o}C. The supernatant was filtered through a 0.2 um cellulose acetate membrane syringe filter and stored in 45 mL light sensitive centrifuge tubes at 4 ^{o}C.

E. coli (ATCC 11229) was propagated as specified in the ATCC material data sheet. For each experiment, 0.2 mL of *E. coli* (ATCC 11229) stock was added to 50 mL nutrient broth and placed in an incubator shaker at 37 ^{o}C for 18-24 hours. After incubation, 10 mL of broth was added to two sterile centrifuge tubes and centrifuged at 5,000 rpm for 5 minutes. Unlike the bacteriophages, *E. coli* 11229 was kept at room temperature throughout experiments and during centrifugation. The liquid in both tubes was then poured out and 10 mL of sterile PBS was added to the tube and shaken. The process of centrifugation and washing with PBS was repeated and the resulting solution was diluted in PBS to produce a concentration of approximately $1x10^{8}$ cfu/mL for the irradiation experiments. After irradiation, the necessary dilutions were spread on nutrient agar plates in 0.1 mL volumes and allowed to dry. The plates were incubated upside down at 37 ^{o}C for 18-24 hours. Each sample was plated in triplicate and plates yielding 0-200 colonies were counted.

Table 4.2. Microorganism Specifications

Microorganism	E. coli Host	Broth	Agar	Solution
MS-2 (15597-B1)	ATCC 15597	tryptone	tryptone	saline-calcium
T7	ATCC 11303	TSB and 0.5% NaCl	tryptone	PBS
E. coli (11229)	N/A	nutrient	nutrient	PBS

4.3 RESULTS AND DISCUSSION

Comsol Model

Comsol Multiphysics was utilized to determine the optimal LED configurations while minimizing the overall cost for the 255 nm and 275 nm LEDs by predicting the Petri factor and average irradiance value for each configuration. For the 255 nm setup, 8 UV-LEDs were used to account for a low power output. The analyzed configurations for the 255 nm setup were labeled the X-Array, 4x2, 8 Evenly Spaced, 3 Rows, and 2x2 With Corners (Figure 4.2). The 275 nm setup consisted of 4 UV-LEDs. The analyzed configurations for the 275 nm setup shown in Figure 4.3 were labeled the Original Array, 4 Corners, 4 Line Array, 4 Staggered Line, and 4 Diagonal. Figure 4.5 and Figure 4.6 display the predicted Petri factor and average irradiance for the compared arrays at a range of distances from the 255 nm UV-LEDs and 275 nm UV-LEDs, respectively.

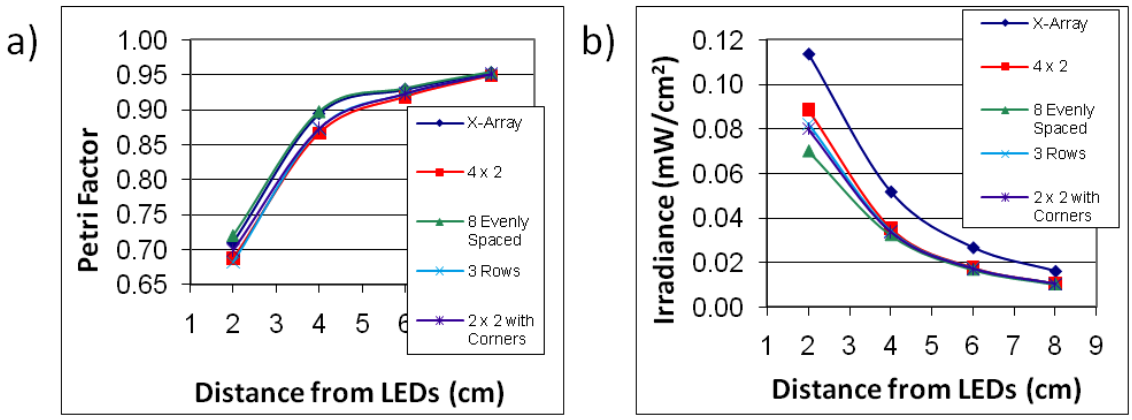

Figure 4.5. Comsol Output: a) Petri factor and b) Irradiance values for 255 nm configurations

The results in Figure 4.5a show that there was not a major difference in the Petri factor between arrays analyzed for the 255 nm configuration. However, the 8 Evenly Spaced and the X Array produced a slightly higher Petri factor than the rest of the arrays for the majority of distance ranges analyzed. Also, both the 8 Evenly Spaced and X Array configurations reached the optimal minimum Petri factor of 0.9 at 4 cm away from the LEDs. The Comsol model output for the irradiance values (Figure 4.5b) shows that X-Array produced the highest average irradiance values for all analyzed distances from the LEDs and the 8 Evenly Spaced configuration produced the lowest. Therefore, the X-Array was selected as the optimal configuration for the 255 nm UV-LEDs due to its higher Petri factor and irradiance values in the simulated Comsol collimated beam apparatus.

The Comsol output for the analyzed 275 nm configurations (Figure 4.6a) shows that the simulated Four Corners array had the highest Petri factor for the entire range of analyzed distances while the other 275 nm arrays produced similar Petri factors for the same range. The 275 nm configuration output (Figure 4.6b) also shows that the Original Array had much higher irradiance values than the other arrays for close distances to the simulated UV-LEDs. For distances beyond 4 cm, the Original Array irradiance results started to converge with the results from the other arrays. The optimal configuration was determined to be a hybrid between the Original and Four Corners arrays formed by increasing the distance between the LEDs in the Original array displayed as Spaced Original in Figure 4.6. The Spaced Original configuration provided higher Petri factor values than the Original Array while still maintaining high irradiance values. Figure 4.7 displays the final configurations for the 255 nm and 275 nm UV-LEDs within the metal LED holders.

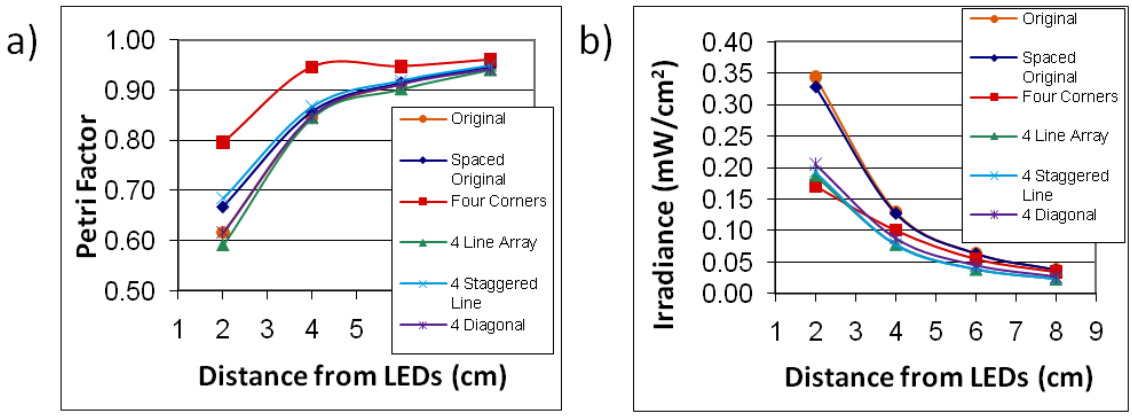

Figure 4.6. Comsol Output: a) Petri factor and b) Irradiance values for 275 nm configurations

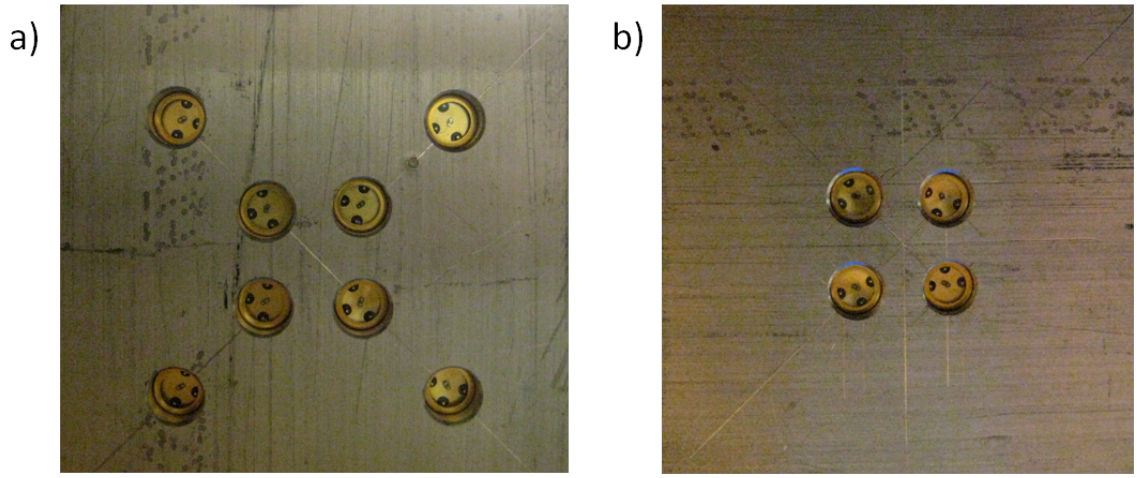

Figure 4.7. Selected Configurations for the a) 255 nm and b) 275 nm UV-LED Arrays

After the UV-LED collimated beam was constructed, irradiance measurements for the 255 nm and 275 nm UV-LED configurations were performed with a Stellarnet EPP2000C Spectrometer and compared to Comsol model output at a range of distances from the UV-LEDs. A comparison of the experimental and model Petri factors for both configurations at a range of distances is presented in Figure 4.8a. Figure 4.8b shows that for the 255 nm UV-LED configuration, the model over predicted the Petri factor at a close range, but approached the experimental value at distances greater than 4 cm from the light source. The opposite occurred with the 275 nm configuration, where the model under predicted Petri factors at small distances from the UV-LEDs and converged with the experimental values at distances greater than 4 cm.

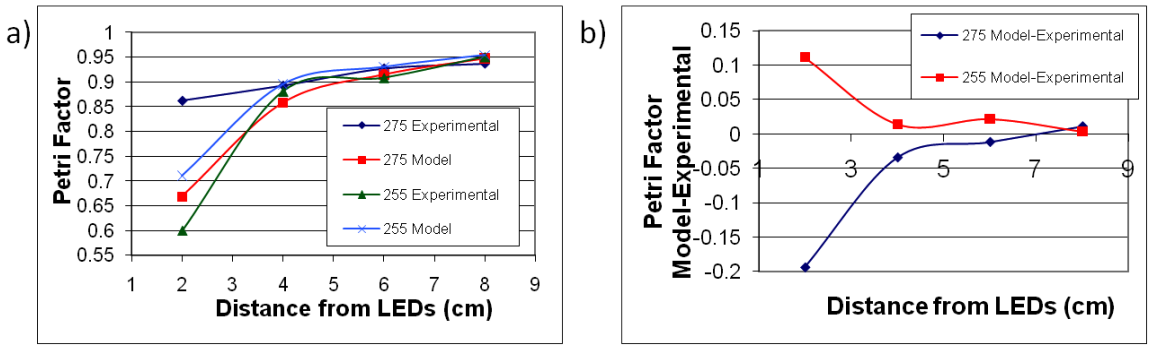

Figure 4.8. a) Model and Experimental Petri Factor Comparison for 275 nm and 255 nm b) Model Petri Factor - Experimental Petri Factor for 275 nm and 255 nm

The model and experimental average irradiance values were compared for the 255 nm and 275 nm configurations in Figure 4.9a. The analysis indicates good agreement between the model and experimental average irradiance values for the 255 nm and 275 nm configurations over the entire range of distances analyzed. Figure 4.9b displays that at the extreme distances (i.e. very close and very far away) the 275 nm UV-LED model predicted slightly higher values than was shown in the experimental data. The 255 nm UV-LED model predicted average irradiance values very similar to the experimental data at a close distance to the UV-LEDs and predicted slightly lower irradiance values at farther distances.

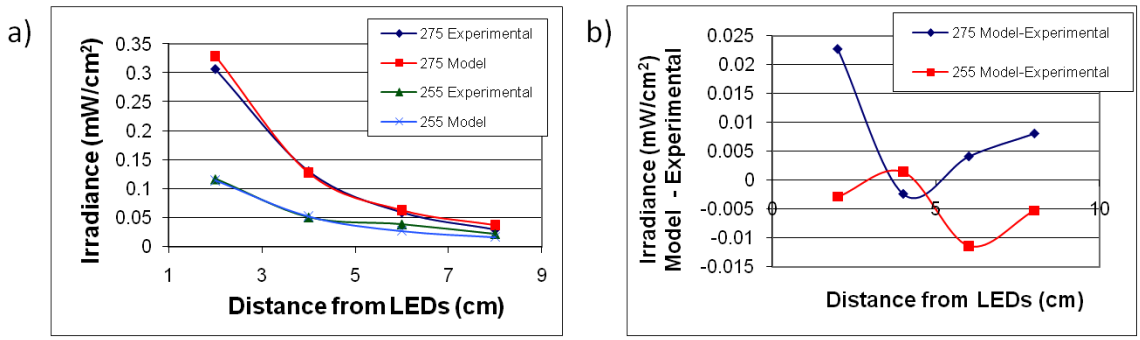

Figure 4.9. a) Model and Experimental Average Irradiance Value Comparison for 275 nm and 255 nm b) Model Irradiance – Experimental Irradiance for 275 nm and 255 nm

All 255 nm and 275 nm UV-LED collimated beam experiments were completed at a 4 cm distance from the UV source. Additional analysis was completed at this distance to determine the difference in model and experimental irradiance values at each individual point over the entire sample area. Figure 4.10 displays the comparison of irradiance values for the 255 nm UV-LED configuration, showing that the majority of the sample area contained less than a 20% variation between model and experimental. A small section in the bottom left edge of the sample contained a 20 to 40% variation between the model and experimental irradiance values for the 255 nm UV-LEDs.

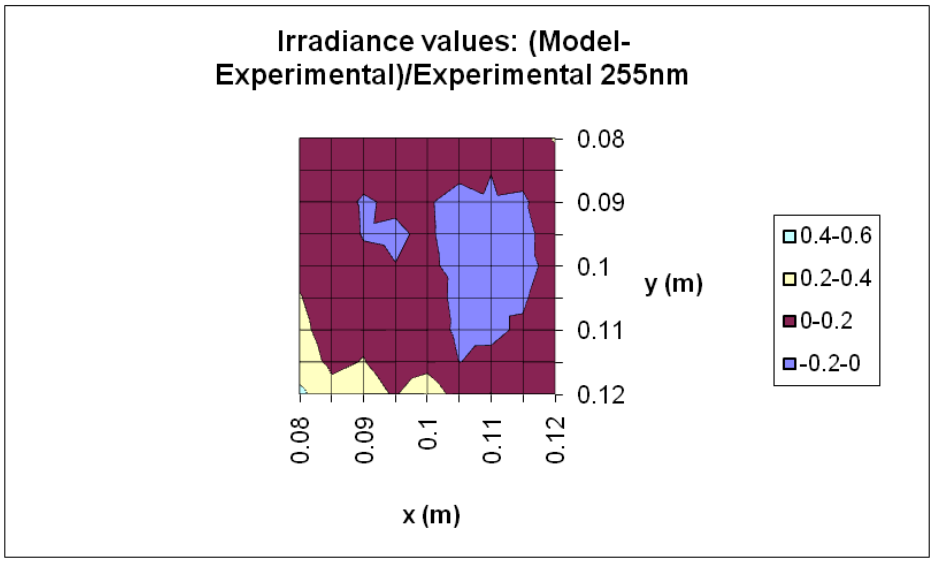

Figure 4.10. Comparison of Model and Experimental Irradiance values for 255 nm UV-LEDs (4 cm distance)

Figure 4.11 displays the fractional difference between model and experimental irradiance values over the sample area at a 4 cm distance for the 275 nm UV-LED setup. Most of the sample area had less than a 10% difference in irradiance between model output and experimental data. The majority of the remaining area had less than a 20% discrepancy between experimental and model irradiance values for the 275 nm UV-LEDs.

The results of these model and experimental UV irradiance comparisons suggest that the model did not include all of the physics inside the collimated beam apparatus. It is hypothesized that the absence of the collimator tube from the model caused a slight shadow zone from the outer edge to some of the UV-LEDs. Consequently, the model would over-predict the contribution of the UV irradiance from these partially blocked

UV-LEDs in these regions. In addition, the presence of the collimator tube was designed to eliminate the divergence of the UV light rays from the emission source. Since the divergence was allowed to occur from the modified point source in Equation 4.2, then the model would tend to underpredict the UV irradiance received at the sample surface.

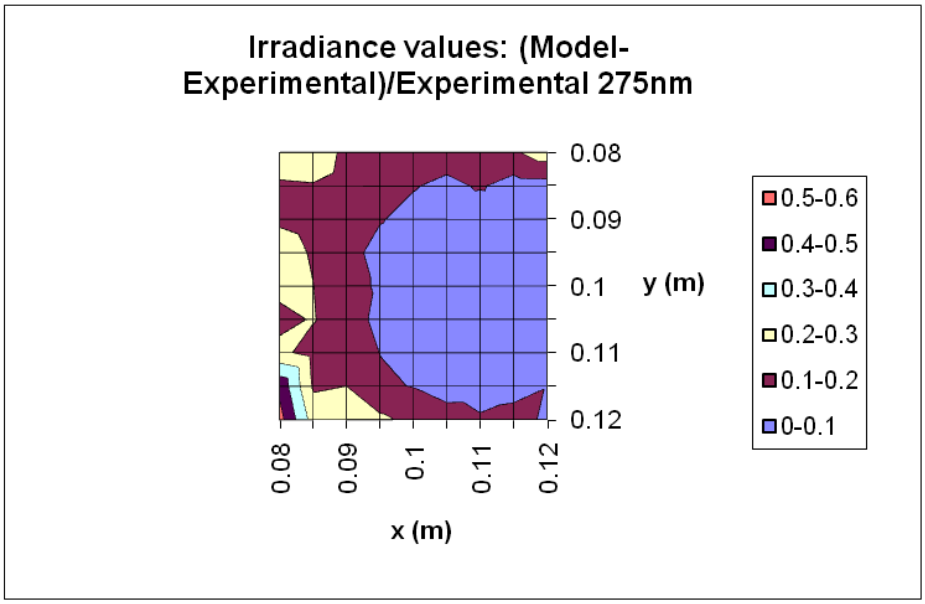

Figure 4.11. Comparison of Model and Experimental Irradiance values for 275 nm UV-LEDs (4 cm distance)

E. coli 11229

Bench scale collimated beam experiments were completed on *E. coli* 11229 using 255nm UV-LEDs, 275 nm UV-LEDs, and low-pressure mercury lamps as the UV light sources. Figure 4.12 displays the results of these experiments in the form of *E. coli* UV fluence-response curves for each UV light source. The curves for all three UV light sources have similar shapes, with a shoulder at the lower UV fluences. The 255 nm LED

results show significantly lower log inactivations than the low-pressure mercury lamp experiments. According to the UV absorption curve for DNA, this is unexpected since the 255 nm LEDs and low-pressure mercury lamps emit at very close wavelengths of 255 nm and 254 nm, indicating a similar germicidal effectiveness (Kalisvaart, 2004). However, it has been proven previously that a UV fluence produced with a low irradiance and a high exposure time may result in lower inactivation rates for *E. coli* when compared to a UV fluence produced with a high irradiance and low exposure time (Sommer et al., 1998; Harm, 1980). The 255 nm UV-LEDs provide a much lower power output than the low-pressure mercury lamps, resulting in lower incident irradiance values (Table 4.1). Therefore, the lower irradiance values may be causing the lower inactivation rates produced in the 255 nm LED experiments compared to the low-pressure mercury lamp experiments.

Sommer et al. (1998) mentioned that higher inactivation rates from high irradiance values combined with low exposure times might be due to repair enzymes that are more susceptible to high UV intensities. However, for a similar range of lower irradiance values and the same UV doses, our study with UV-LEDs at 255 nm resulted in much lower *E. coli* inactivations than Sommer et al. (1998), who used low-pressure mercury lamps. For the higher UV intensity experiments where both Sommer et al. and our study used low-pressure mercury lamps, the UV dose-response kinetics for the studies were very similar. A decrease in UV irradiance from low-pressure mercury lamps in Sommer et al. (1998) at a UV fluence of 7 mJ/cm^2 resulted in a slight *E. coli* log

inactivation decrease from 3.97 to 3.65. A similar decrease in UV irradiance values from the low-pressure mercury lamps to the 255 nm LED experiments in our study resulted in a log inactivation decrease from 3.76 to 1.68. Therefore, the change in UV light intensity may not be the only factor in the difference in UV response kinetics between the low-pressure and 255 nm LED experiments. If the photon absorption is different in the UV-LED experiments than the low-pressure mercury lamp experiments, this could also partially explain the difference in the UV dose-response kinetics between the two UV light sources. Wayne (1999) hypothesized that the higher microbial inactivations resulting from high irradiance values and low exposure times could also be due to the higher UV intensities causing simultaneous photon absorption in a shorter exposure time as opposed to lower UV intensities with higher exposure times causing sequential photon absorption.

The 275 nm UV-LED experiments produced higher *E. coli* 11229 inactivation rates than the 255 nm experiments (Figure 4.12), despite the UV absorption curve for DNA showing a lower absorption for 275 nm (Kalisvaart, 2004). The larger *E. coli* inactivation in the 275 nm UV-LED experiments compared to the 255 nm UV-LED experiments may be due to the higher power output of the 275 nm UV-LEDs, resulting in higher irradiance values and shorter exposure times to reach the same UV fluence as discussed in the results for the 255 nm UV-LEDs. Another contributing factor for the 275 nm LED irradiation providing higher inactivation rates than 255 nm UV-LEDs may be the absorption spectra of proteins reaching a peak around 280 nm, meaning that repair

enzymes are more prone to damage from UV irradiation at wavelengths near 280 nm (Kalisvaart, 2004).

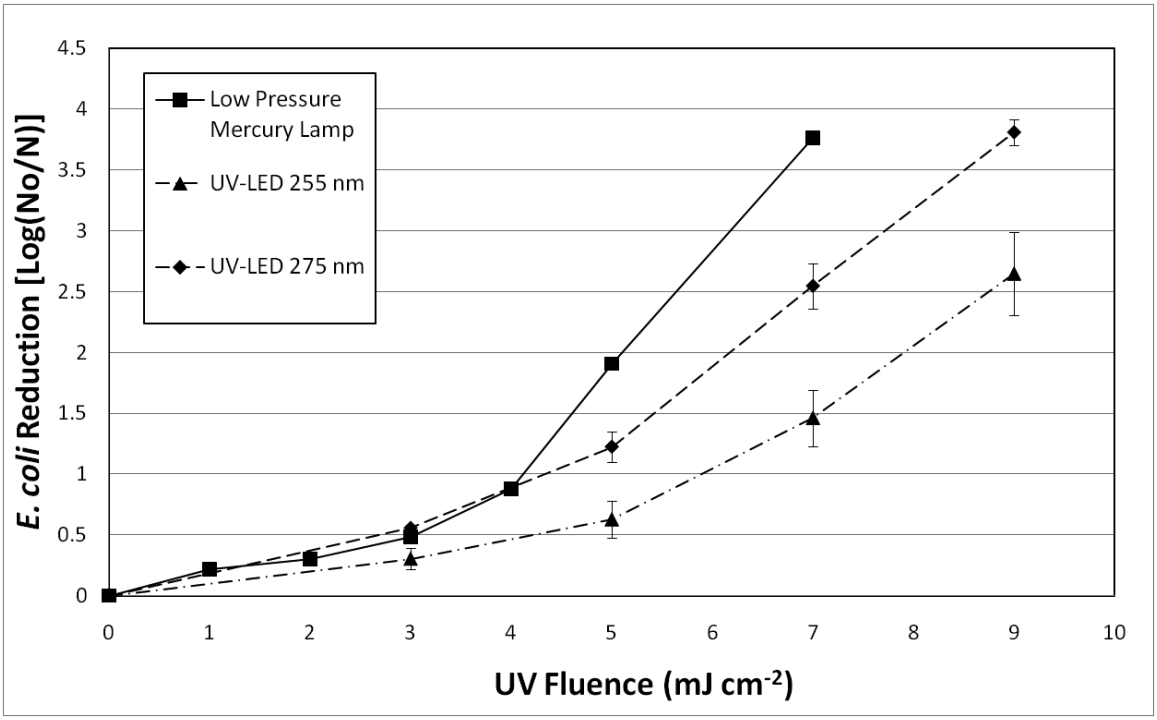

Figure 4.12. UV Fluence-Response Curves for *E. coli*

MS-2 Bacteriophage

The MS-2 UV fluence-response curves for all UV light sources resulted in a log-linear relationship. Like the results for *E. coli* 11229, MS-2 bacteriophage had lower reduction rates for the 255 nm UV-LED experiments than for the low-pressure mercury lamp experiments as is displayed in Figure 4.13. However, the decrease in inactivation rates from low-pressure to 255 nm UV-LEDs was much smaller than with the *E. coli* experiments. Sommer et al. (1998) saw no significant change in MS-2 response kinetics

from high intensity-low exposure time to low intensity-high exposure time for the same UV fluence. Therefore, the decrease in inactivation may not be a result of the decrease in UV intensity from low-pressure mercury lamps to UV-LEDs emitting at 255 nm. Figure 4.13 shows that the 255 nm LED results are almost within the expected range for MS-2 UV fluence-response kinetics due to low-pressure mercury lamp irradiation as specified by the US EPA UV Disinfection Guidance Manual (USEPA, 2006). Therefore, it may also be argued that the difference in the MS-2 UV fluence-response kinetics between the low-pressure mercury lamp and 255 nm LED experiments is not significant.

The experiments with UV-LEDs emitting at 275 nm resulted in very similar UV dose response kinetics to the 255 nm LED experiments with slightly lower inactivations at higher UV doses. The spectral sensitivity of MS-2 displays a peak around 260 nm, which may explain the slightly higher inactivation for 255 nm compared to 275 nm LEDs (Mamane-Gravetz et al., 2005).

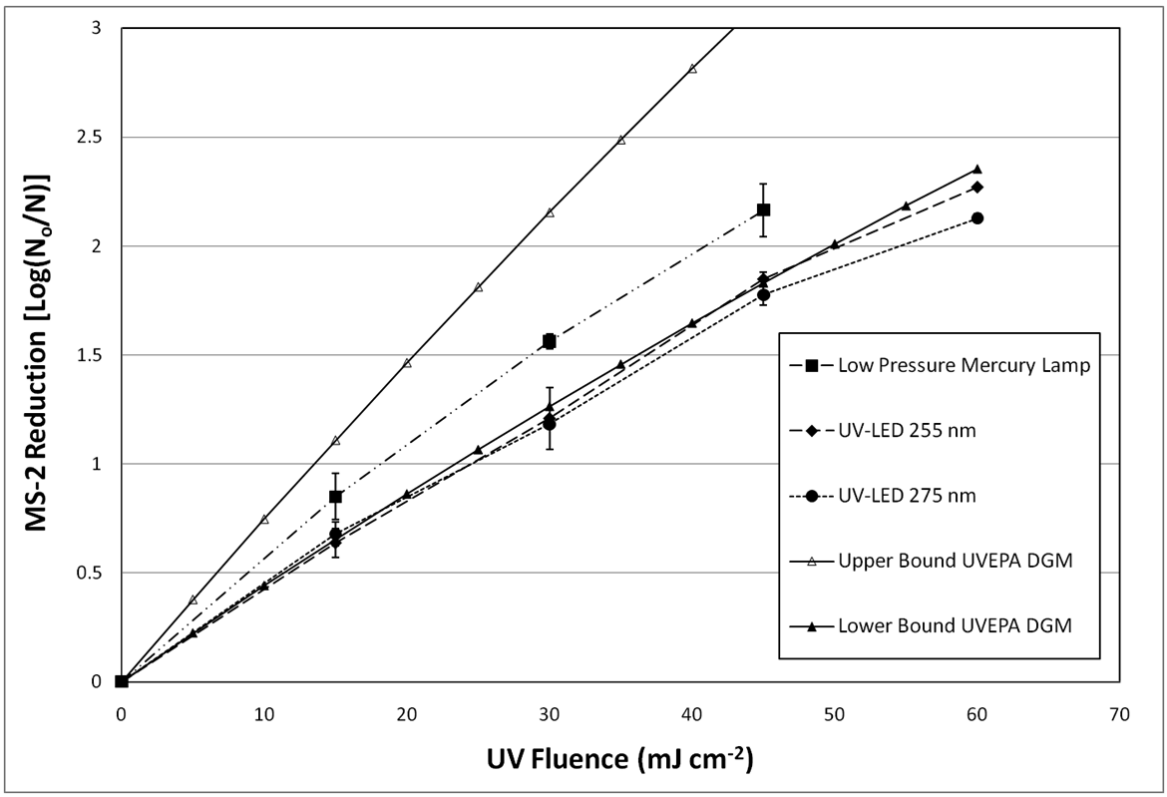

Figure 4.13. UV Fluence-Response Curves for MS-2 Bacteriophage

T7 Bacteriophage

T7 bacteriophage experiments resulted in slightly lower inactivation values for the same UV fluences with irradiation by 255 nm UV-LEDs compared to low-pressure mercury lamp irradiation (Figure 4.14). Time-dose reciprocity experiments for T7 are not readily available in the literature so it is not clear whether the lower inactivation rates for 255 nm UV-LEDs are due to the lower UV intensity from the UV-LEDs compared to the low-pressure mercury lamps or to some other phenomenon. However, since T7 and MS-2 are both bacteriophages, it is possible that these microorganisms would behave

similarly in terms of following the time-dose reciprocity law, meaning that the lower irradiance values would not produce lower inactivation rates.

Unlike MS-2, the T7 275 nm LED experiments resulted in very similar UV fluence-response kinetics to the low-pressure mercury lamp results and a slightly higher log inactivation for each UV fluence when compared to the 255 nm UV-LED experiments (Figure 4.14). The action spectrum of T7 displays a small peak around 270 nm, which may explain the increased inactivation by the 275 nm UV-LEDs compared to the 255 nm UV-LEDs (Ronto et al., 1992).

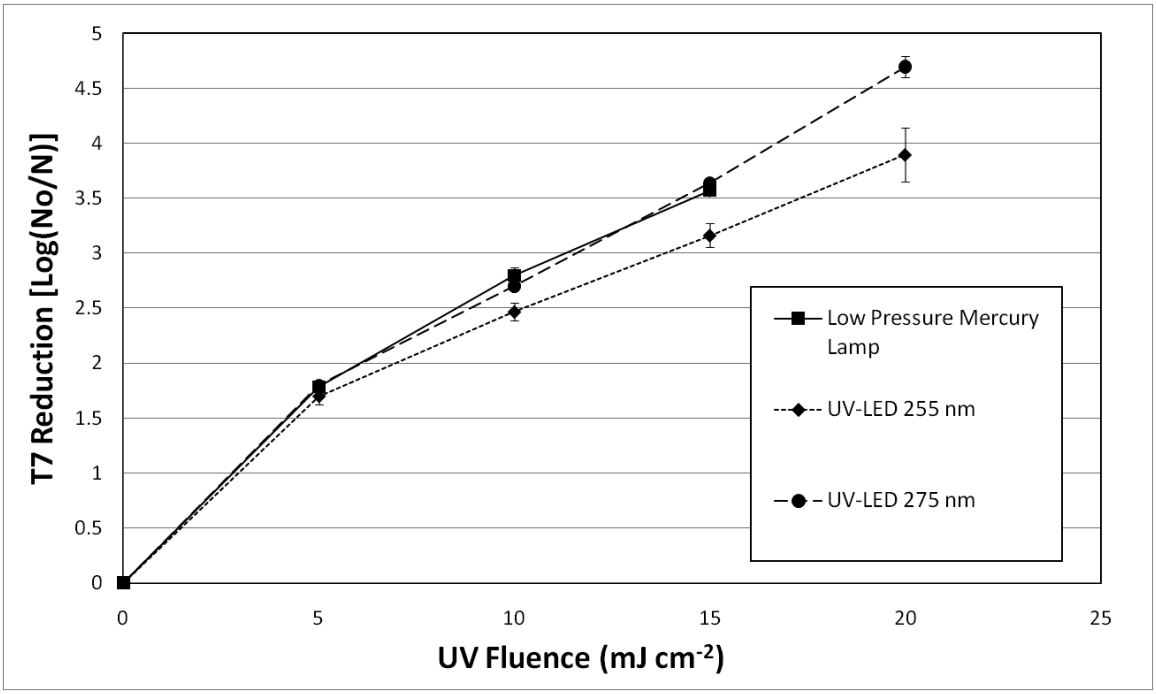

Figure 4.14. UV Fluence-Response Curves for T7 Bacteriophage

4.4 CONCLUSION

This study compared the UV fluence-response of MS2, T7, and *E. coli* 11229 when exposed to low-pressure mercury lamps emitting at 254 nm and UV-LEDs emitting at 255 nm and 275 nm. *E. coli* 11229 inactivation was most efficient in the low-pressure mercury lamp experiments and the least efficient for the 255 nm UV-LED experiments. MS-2 had very similar UV fluence-response kinetics for all three UV sources, with slightly higher inactivation rates corresponding to low-pressure mercury lamp irradiation. T7 also had similar UV fluence-response kinetics for all UV sources, but responded with slightly lower inactivation rates to irradiation by 255 nm UV-LEDs compared to the inactivation rates for irradiation by low-pressure mercury lamps and 275 nm UV-LEDs.

This research indicates that 275 nm UV-LEDs may produce more efficient microbial inactivation than 255 nm UV-LEDs for T7 and *E. coli* and almost identical microbial inactivation for MS-2. Typically, wavelengths around the peak of DNA absorption (260 nm) are considered to produce the highest disinfection efficiency (Kalisvaart, 2004). Therefore, further investigation should be performed to investigate the UV-LED disinfection trends found in this study and whether they are applicable for a variety of UV irradiances.

The results of this study indicate that UV-LEDs may be suitable for UV disinfection applications as long as steps are taken to determine the UV fluence-response

of target surrogate microorganisms. However, the low UV-LED power output makes very long exposure times necessary to induce significant microbial inactivation. Consequently, until the UV-LED technology is improved to make the power output more efficient, UV-LEDs may best serve the point-of-use, low flow disinfection applications.

5. FUTURE WORK

Future work for this research will include determining the UV fluence curves for T7, MS2, *and E. coli* in response to irradiation by 255 nm UV-LEDs, 275 nm UV-LEDs, and low-pressure mercury lamps with equal UV irradiance values. Constant UV irradiance values can be accomplished by moving the microbial sample further from the higher power light sources (i.e. from either the LP mercury lamp or the 275 nm UV-LEDs) to allow the same incident irradiance for a sample placed closer to the 255 nm UV-LEDs. Results would help determine whether the change in microbial response kinetics between the two UV-LED wavelengths and between the 255 nm UV-LEDs and low-pressure lamps in this study was due to the difference in UV intensity or to some other factor as suggested by researchers and in this study.

6. REFERENCES

Bohrerova, Z., Shemer, H., Lantis, R., Impellitteri, C. A., & Linden, K. G. (2008). Comparative disinfection efficiency of pulse and continuous-wave UV irradiation technologies. Water Research, 42, 2975-2982.

Bohrerova, Z., Mamane, H., Ducoste, J. & Linden, K.G. (2006). Comparative inactivation of Bacillus subtilis spores and MS-2 coliphage in a UV reactor: implications for validation. Journal of Environmental Engineering ASCE, 132, 1554-1561.

Bolton, J. R. (2000). Calculation of ultraviolet fluence rate distributions in an annular reactor: Significance of refraction and reflection. Water Research, 34(13), 3315-3324.

Bolton, J. R., and Linden, K. G. (2003). Standardization of methods for fluence (UV dose) determination in bench-scale UV experiments. Journal of Environmental Engineering, 129(3), 2009-215.

Chung, S., Yang, W., & Krishnamurthy, K. (2008). Effects of Pulsed UV-Light on Peanut Allergens in Extracts and Liquid Peanut Butter. Journal of Food Chemistry, 73(5), 400-404.

Crawford, M., Banas, M., Ross, M., Ruby, D., Nelson, J., Boucher, R., Allerman, A. (2005). Final LDRD report; Ultraviolet water purification systems for rural environments and mobile applications. Sandia Report., <http://www.prod.sandia.gov> (October 26, 2008)

Dume, B. (2006). *LEDs Move into the Ultraviolet.* Retrieved Mar. 25, 2010, from Physics World, Bristol, UK. Web site: http://physicsworld.com/cws/article/news/24926.

Fallon, K. S., Hargy, T. M., Mackey, E. D., & Wright, H. B. (2007). Development and characterization of nonpathogenic surrogates for UV reactor validation. *Journal AWWA*, *99*(3), 73-82.

Gates, F. L. (1929). A study of the bactericidal action of ultra violet light. *Journal of General Physiology*, *13*, 231-248.

Harm, W. In Biological effects of ultraviolet radiation; Cambridge University Press: New York, 1980.

Kalisvaart, B. F. (2004). Re-use of wastewater: Preventing the recovery of pathogens by using medium-pressure UV lamp technology. *Water Science and Technology*, *50*(6), 337-344.

Linden, K. G., Shin, G., & Sobsey, M. D. (2001). Comparative effectiveness of UV wavelengths for the inactivation of *Cryptosporidium parvum* oocysts in water. *Water Science and Technology*, *43*(12), 171-174.

Liu, D., Ducoste, J., Shanshan, J., & Linden, K. (2004). Evaluation of alternative fluence rate distribution models. *Journal of Water Supply: Research and Technology-AQUA*, *53*(6), 391-408.

Malley, J. P., Ballester, N. A., & Margolin, A. B. (2004). *Inactivation of Pathogens with Innovative UV Technologies.* Denver, CO: AWWA Research Foundation.

Mamane-Gravetz, H., Linden, K. G., Cabaj, A., & Sommer, R. (2005). Spectral Sensitivity of *Bacillus subtilis* Spores and *MS2 Coliphage* for Validation Testing of Ultraviolet Reactors for Water Disinfection. *Environmental Science and Technology*, *39*, 7845-7852.

Mori, M., Hamamoto, A., Takahashi, A., & Nakano, M. (2007). Development of a new water sterilization device with a 365 nm UV-LED. *Med Bio Eng Comput*, *45*, 1237-1241.

Rahn, R. O. (1997). Potassium Iodide as a Chemical Actinometer for 254 nm Radiation: Use of Iodate as an Electron Scavenger. *Photochemistry and Photobiology*, *66*(4), 450-455.

Rahn, R. O., Stefan, M. I., Bolton, J. R., & Goren, E. (2003). Quantum Yield of the Iodide-Iodate Chemical Actinometer: Dependence on Wavelength and Concentration. *Photochemistry and Photobiology*, *78*(2), 146-152

Ronto, G., Gaspar, S., & Berces, A. (1992). Phages T7 in biological UV dose measurement. *Journal of Photochemistry and Photobiology B: Biology*, *12*(3), 285-294.

(2008). *S-ET, Inc. UVTOP Technical Data.* Retrieved Sep. 25, 2009, from Sensor Electronic Technology (S-ET, Inc.), Columbia, SC. Web site: http://www.s-et.com/

Shur, M. S. and R. Gaska. (2008). III-nitride based deep ultraviolet light sources. Proc. SPIE Vol. 6894., San Jose, CA, USA.

Sommer, R., Haider, T., Cabaj, A., Pribil, W., and Lhotsky, M. (1998). Time dose reciprocity in UV disinfection of water. *Water Science and Technology*, 38(12), 145-150.

U.S. Environmental Protection Agency (USEPA). (2006). Ultraviolet disinfection guidance manual. Washington, D.C., <http://www.epa.gov/safewater/lt2/pdfs/guide_lt2_uvguidance_draft.pdf> (October 21, 2008).

Vilhunen, S. H., Sarkka, H., & Sillanpaa, M. (2009a). Ultraviolet light-emitting diodes in water disinfection. *Environ Sci Pollut Res*, *16*, 439-442.

Vilhunen, S. H., & Sillanpaa, M. E. (2009b). Ultraviolet light emitting diodes and hydrogen peroxide in the photodegradation of aqueous phenol. *Journal of Hazardous Materials*, *161*, 1530-1534.

Vilhunen, S. H., Rokhina, E. V., & Virkutyte, J. (2010). Evaluation of UV-LEDs Performance in Photochemical Oxidation of Phenol in the Presence of H2O2. *Journal of Environmental Engineering*, *136*(3), 274-280.

Wang, T., MacGregor, S. J., Anderson, J. G., & Woolsey, G. A. (2005). Pulsed ultra-violet inactivation spectrum of Escherichia coli. *Water Research*, 39, 2921-2925.

7. APPENDIX

7.1 APPENDIX A - Checklist for UV-LEDs and Stellarnet Spectrometer

Turning on the UV-LEDs

1) Place UV TOP LEDs (SET, Inc.) into metal holder

2) Place thin metal plate over LEDs, taking care to keep anodes and cathodes away from the plate edge. Make sure that the screws are not too tight.

3) Put LED holder into the collimated beam box. Attach the blue wire from the bread board to the cathode and ground and the red wire to the anode for all LEDs. Be very careful with the LEDs. The cathode, anode, and ground can be broken easily.

4) Connect the black plug of the cord to the negative symbol on the Agilent 6614C power supply and the red segment of the cord to the positive symbol on the power supply. On the bread board, red cord attached to power supply goes to the red line and black cord goes to the blue line.

5) Turn on power supply by pressing the line switch.

6) Press voltage, enter 14.5 V, press enter. Press current. For 4 LEDs, type in 0.08 (or 80 mA). For 8 LEDs, type 0.16 (or 160 mA). This sends 20 mA to each LED. Press enter. To send the power to the LEDs, press Output on/off.

7) To turn off LEDs, press Output on/off. To turn off power supply, press line.

Stellarnet Spectroradiometer

1) Connect CR2-RA (sensor box) to the Stellarnet EPP2000C spectrometer using the F600-UVVis-SR fiber cord. Connect Stellarnet spectrometer to the computer using the USB2EPP cable into the right USB port. Also connect Stellarnet spectrometer to power supply using UP5V cord.

2) Open SpectraWiz software on computer. To put the software into radiometer mode, go to View→Radiometer→uW/flux and Irradiant uW/cm^2

3) To set wavelength range for power measurement:

   View→Radiometer→Setup range for Watt and Rflux measurement

   Be sure to capture all of the wavelengths that the UV device is outputting. For example, the 255 nm UV-LEDs output from approximately 230 nm to 275 nm.

7.2 APPENDIX B - Ingredients for Broth, Agar, and Solutions

Tryptone bottom agar

- 10 g tryptone
- 1 g yeast
- 8 g NaCl
- 15 g Bacto agar
- 1 g glucose
- 2 mL $CaCl_2$ (1 M concentration)
- 1000 mL DI water

Tryptone top agar

- 2 g tryptone
- 0.2 g yeast
- 1.6 g NaCl
- 2 g Bacto agar
- 0.2 g glucose
- 0.4 mL $CaCl_2$ (1 M concentration)
- 200 mL DI water

TSB with 0.5% NaCl

- 3 g TSB (tryptic soy broth)
- 0.5 g NaCl
- 100 mL DI water

Tryptone broth

- 1 g tryptone
- 0.1 g yeast
- 0.8 g NaCl
- 0.1 g glucose
- 0.2 mL $CaCl_2$ (1 M concentration)
- 100 mL DI water

Saline-calcium Buffer

- 1.7 g NaCl
- 0.4 mL $CaCl_2$ (1 M concentration)
- 200 mL DI water

Nutrient broth, Nutrient agar, and Phosphate Buffer Saline (PBS) were bought pre-prepared. PBS was diluted as necessary.

7.3 APPENDIX C - Average UV fluence determination (Bolton and Linden, 2003)

Correction factors

1. Reflection Factor:

Reflection factor accounts for the reflection when the beam comes from one media to another. For air and water, reflection factor is 0.975, and represents the fraction of the incident beam that enters the water.

2. Petri Factor

Petri factor is defined as the ratio of the incident irradiance average over the Petri dish area to the irradiance at the center of the dish and is used to correct the irradiance reading at the center of the Petri dish to more accurately reflect the average incident fluence rate over the surface area.

i) Scan the radiometer over every grid in the area of the Petri dish using the horizontal direction as the x-axis and the vertical direction as the y-axis. Be sure to include grids on the slope between the axes (for example (1,1) or (2,2)).

ii) Divide the irradiance at each point by the center irradiance to be the ratio value.

iii) Take the average of the all the ratios to equal the Petri Factor.

In general, a well designed collimated beam apparatus should deliver a Petri Factor

greater than 0.9.

3. Water Factor

Water factor accounts for the decrease in irradiance from absorption as the beam passes through the water.

$$Water\ Factor = \frac{1-10^{-a\ell}}{a\ell \ln(10)}$$

a: absorbance for a 1cm path length at the wavelength that is emitted by the UV light source (254 nm for the low-pressure mercury lamp and 255 nm or 275 nm for the UV-LEDs)

ℓ: vertical path length (cm) of the water in the Petri dish.

4. Divergence Factor

$$Divergence\ Factor = \frac{L}{L+\ell}$$

L: distance from the UV lamp to the surface of the cell suspension (cm).

ℓ: vertical path length (cm) of the water in the Petri dish.

Average Fluence calculation:

Fluence = E0 × Petri Factor × Reflection Factor × Water Factor × Divergence Factor × t

E0: radiometer reading at the center of the Petri dish area.

t: exposure time

7.4 APPENDIX D - Iodide/iodate actinometry (Rahn, 1997; Rahn, 2003)

Solutions preparation

Make a 0.01 M borax / 0.1 M potassium iodate / 0.6 M potassium iodide solution by adding 0.38 g of $Na_2B_4O_7 \cdot 10H_2O$, 2.14 g of KIO_3, and 9.96 g KI to 100 L of DI water.

Actinometry Procedure for low-pressure mercury lamp and 255 nm UV-LEDs

1) Determine the pH, adjust to make it 9.25.

2) Add 10 mL of the solution to a 50 × 35 mm Petri dish. Place in position and center under the UV light making sure the water level is at the same distance from the light as the radiometer sensor and leave for 1 min while UV light off. Use DI water as baseline to zero the spectrophotometer. Determine the absorbance at 352 nm and 300 nm. Make sure to use different liquid to determine the absorbance at the two different wavelengths.

3) Add 10 mL of the solution to the 50 × 35 mm petri dish and center under the UV light, making the water level the same as the radiometer sensor level. Do this three times with targeted irradiation times (for example, 30, 45 and 60 s). After irradiating each solution, determine the absorbance at 352nm.

4) Determine the temperature of the solution.

5) Determine the iodide concentration using the following formula:

$$Iodide(M) = \frac{OD(300nm)}{1.061}$$

6) Determine the quantum yield at the irradiating wavelength using the concentration of iodide (C) and the temperature (T) in degrees Celsius

$$\phi = 0.75[1 + 0.02(T - 20.7)][1 + 0.23(C - 0.577)]$$

7) Determine the triiodide concentration using the molar extinction coefficient of 26400 $M^{-1}cm^{-1}$ for 254 nm.

$$Triiodide(M) = \frac{\Delta OD(300nm)}{26400 \;\; M^{-1}cm^{-1}}$$

$$\#\;\; moles \;\; triiodide = triiodide(M) \times volume \;\; of \;\; irradiated \;\; sample$$

8) Determine the UV fluence using the quantum yield and the conversion from einsteins to joules:

$$UV \;\; fluence(\frac{J}{cm^2}) = \frac{\#\;\; moles \;\; triiodide}{\phi \times cross \;\; \sec tional \;\; area(cm^2)} \times 4.72 \times 10^5 \frac{J}{einstein}$$

To find the UV fluence rate, divide by exposure time.

Actinometry Procedure for 275 nm UV-LEDs

1) Complete the same protocol as described for low-pressure mercury lamps with the following exceptions:
    a. Use the quantum yield value of 0.44 and molar extinction coefficient of 27600 $M^{-1}cm^{-1}$ as specified in Rahn (2003) for 274 nm

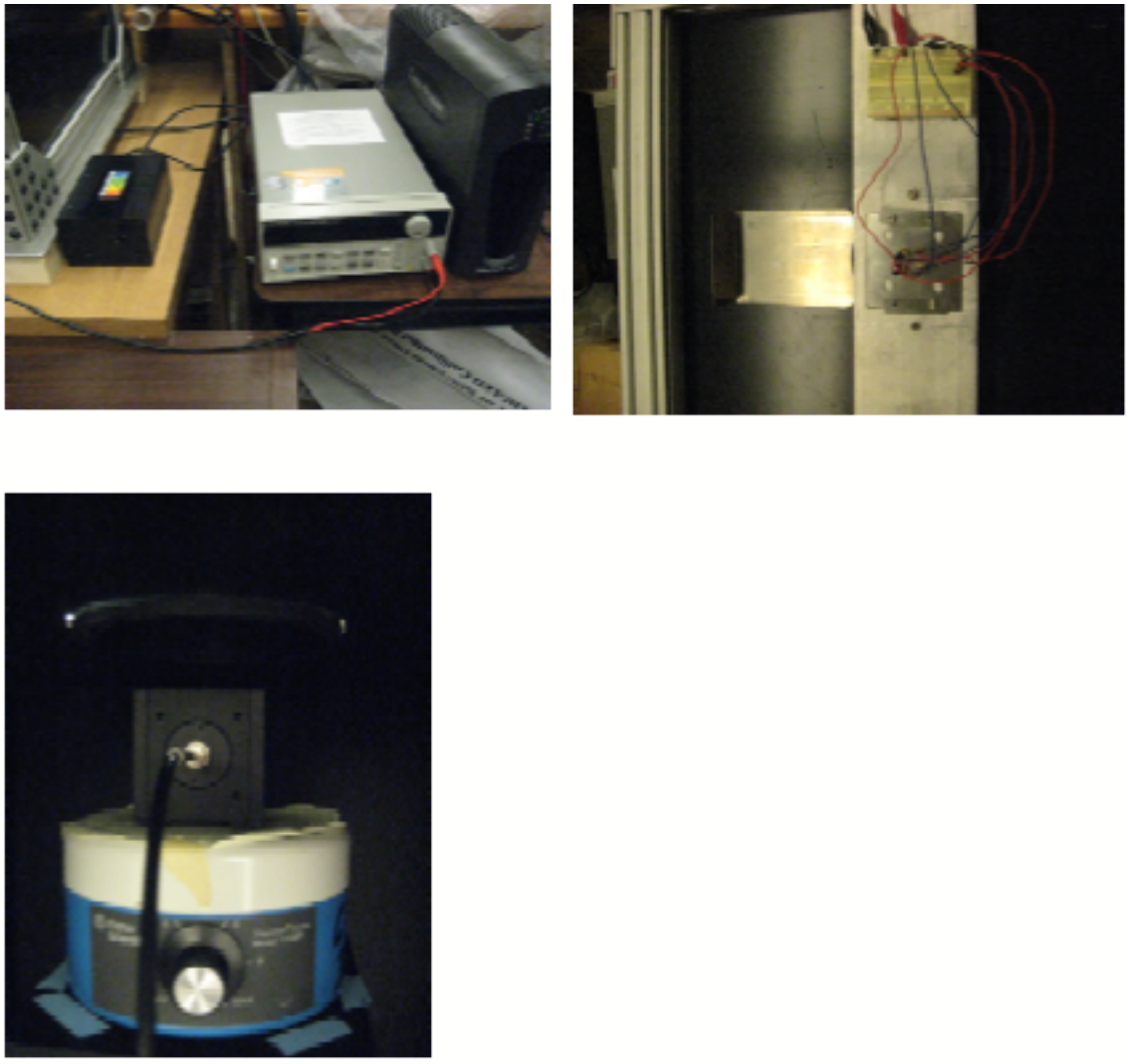

Figure 7.1. a) Stellarnet EPP2000C Spectrometer and Agilent 6614C Power Supply b) Top of UV-LED Collimated Beam with shutter out c) Stellarnet CR2 Sensor

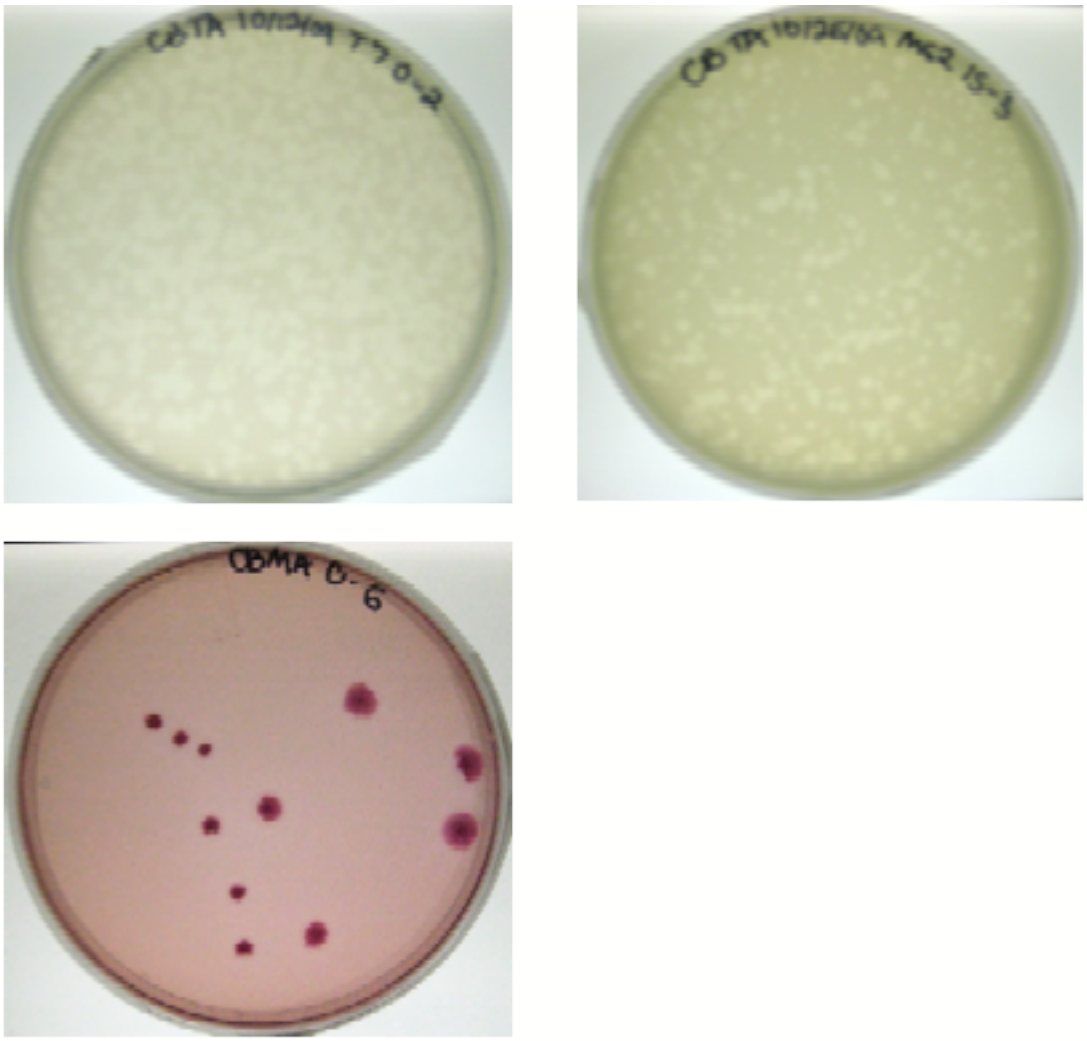

Figure 7.2. T7, MS-2, and *E. coli* Petri dishes